Molecules in the Local Universe

Leslie Hunt
INAF-Osservatorio di Arcetri
Firenze

Why study molecules and the interstellar medium?

- Stars form from dense, cool H_2; *molecules trace star formation*
- The *interstellar medium* plays an important role as the *sink for energy exchange* and provides raw material
- Star formation occurs in dense *dusty clouds* so need some tracer that *penetrates the dust (long wavelengths > 10μm fundamental)*
- Spectral observations also trace kinematics, so can be used to *probe dynamical mass, gas motion, and gravitational torques*

Overview of lectures

I. CO and star formation in galaxies:

ISM energy cycle
HI and H_2 in the ISM
CO as a tracer of H_2
CO morphology in nearby spiral galaxies
Molecular gas and star formation (Kennicutt-Schmidt Law)

II. CO kinematics in galaxies:

Different visualizations of kinematics
Rotation curves
Dynamical resonances
Gravitational torques

III. (Some) Other molecules and metal abundance:

Tracers of dense gas (HCN, HCO^+)
Optically thin molecular tracers (^{13}CO) and column densities
Molecular content in low-metallicity galaxies

I. CO and star formation in galaxies

The interstellar medium energy cycle

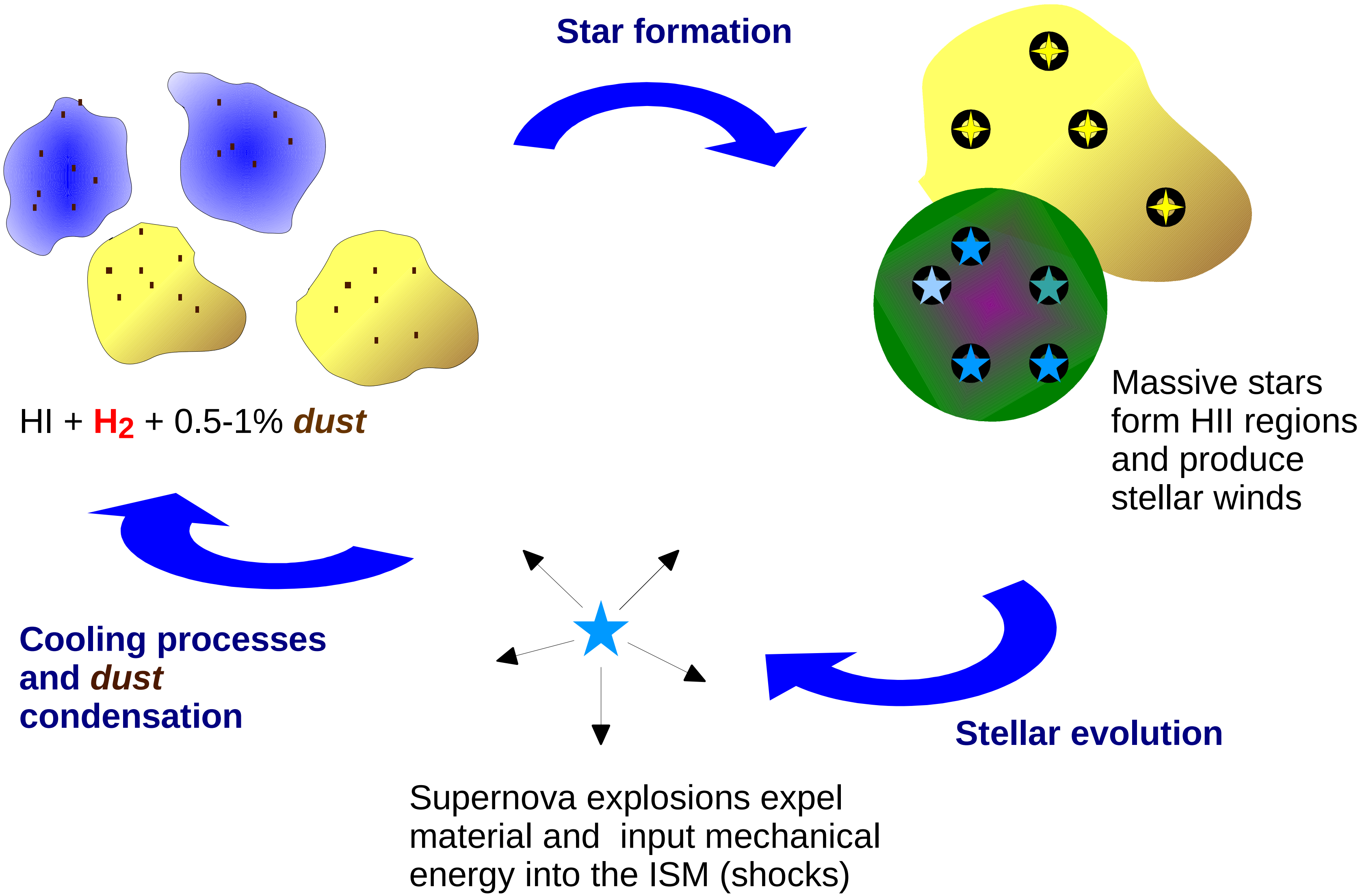

The interstellar medium energy cycle

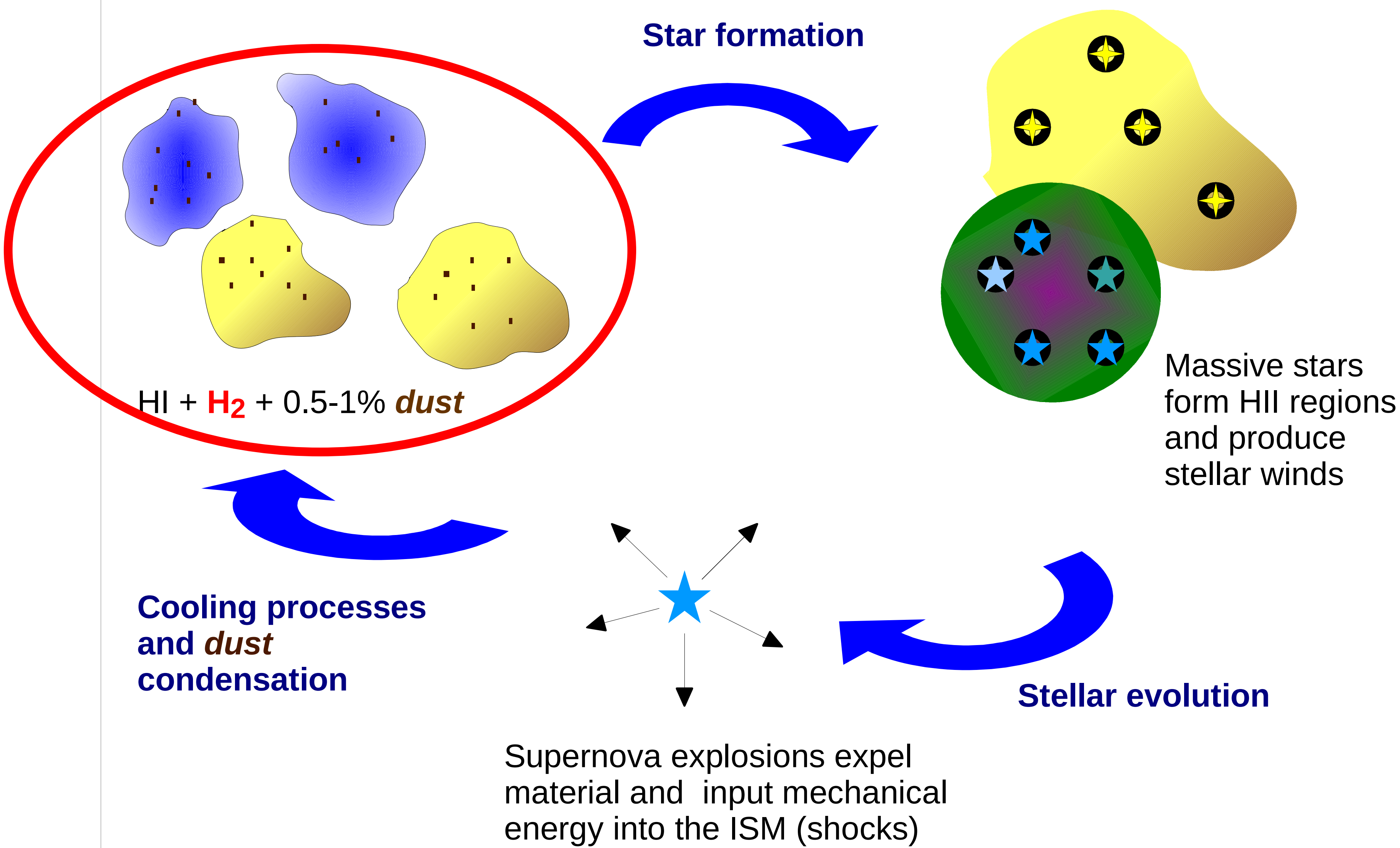

Composition of the ISM

~90% H, ~9% He, <1% dust (metals)

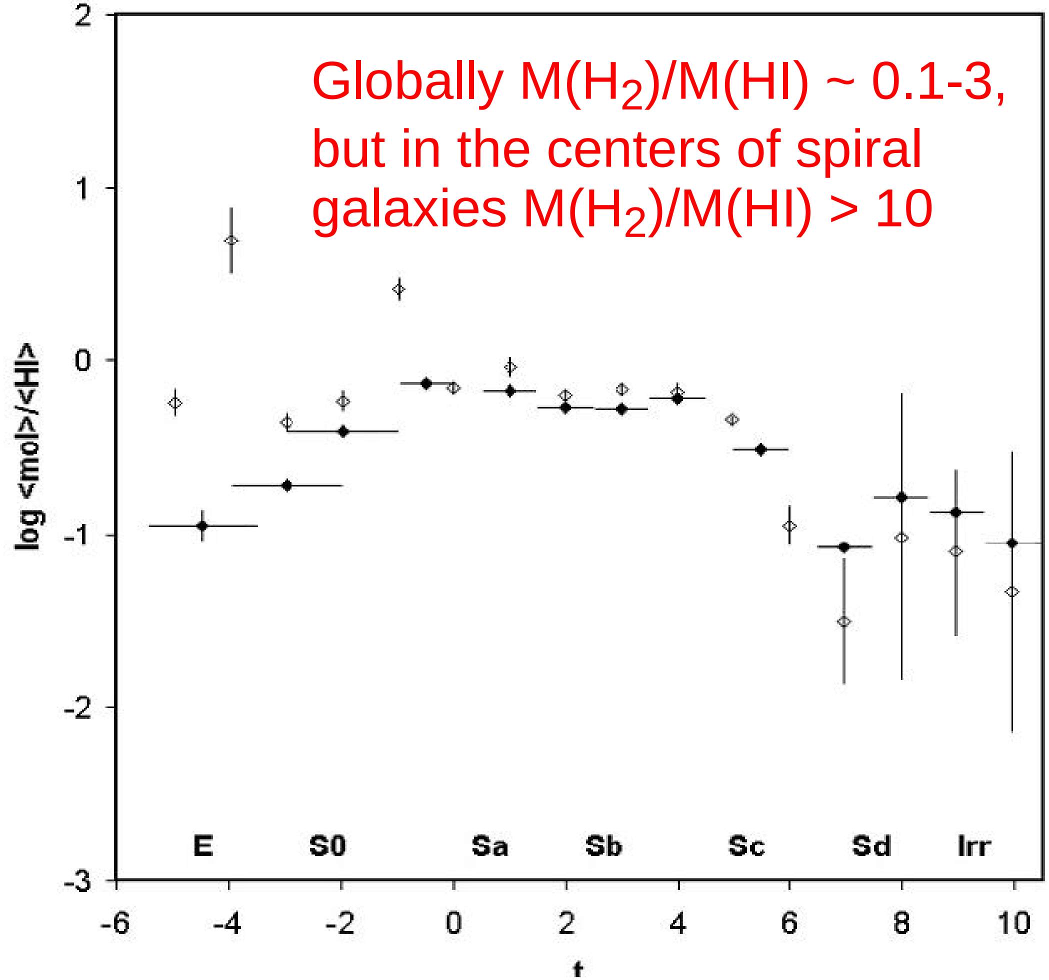

Relative amounts of HI and H_2 depend on galaxy morphological type (Casoli+ 1998, Bettoni+ 2003)

Where is the gas?

HI is usually much more extended than optical and H_2 (CO). The atomic gas (HI) distribution (middle panel) shows a much larger extent than the CO (bottom), or the optical (stellar) disk (top: optical in color, HI in contours) (see Haan+ 2008, 2009).

NOTE: CO traces H_2 which follows the star formation (see coming slides)...

HI and H_2 (CO) follow the exponential stellar disk, but usually with a central HI depression (hole) (see Kenney &Young 1989, Bigiel+ 2008)

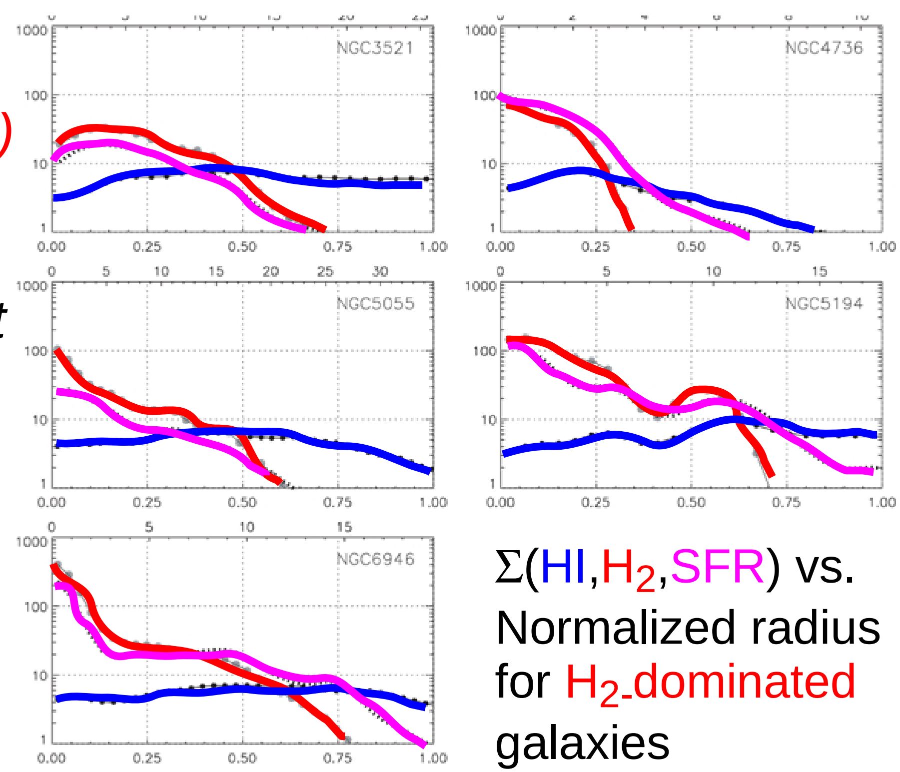

Σ(HI,H_2,SFR) vs. Normalized radius for H_2-dominated galaxies

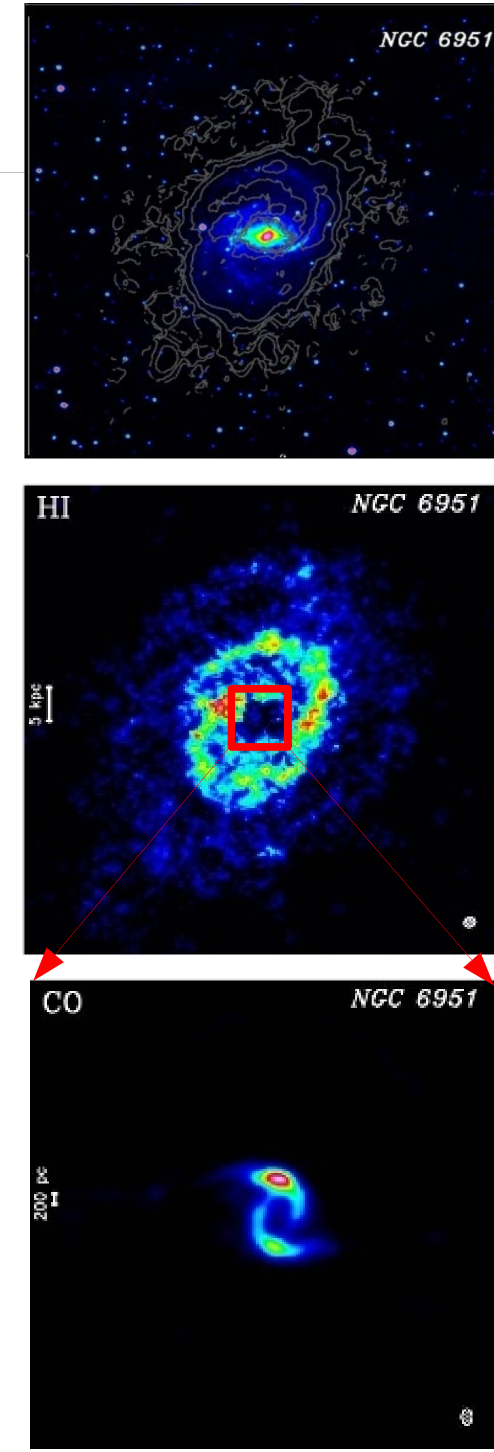

Why don't stars form from atomic hydrogen?

HI emits at 1.42041 MHz (21.1 cm) by radiative transitions between the two hyperfine levels of the ground electronic state.

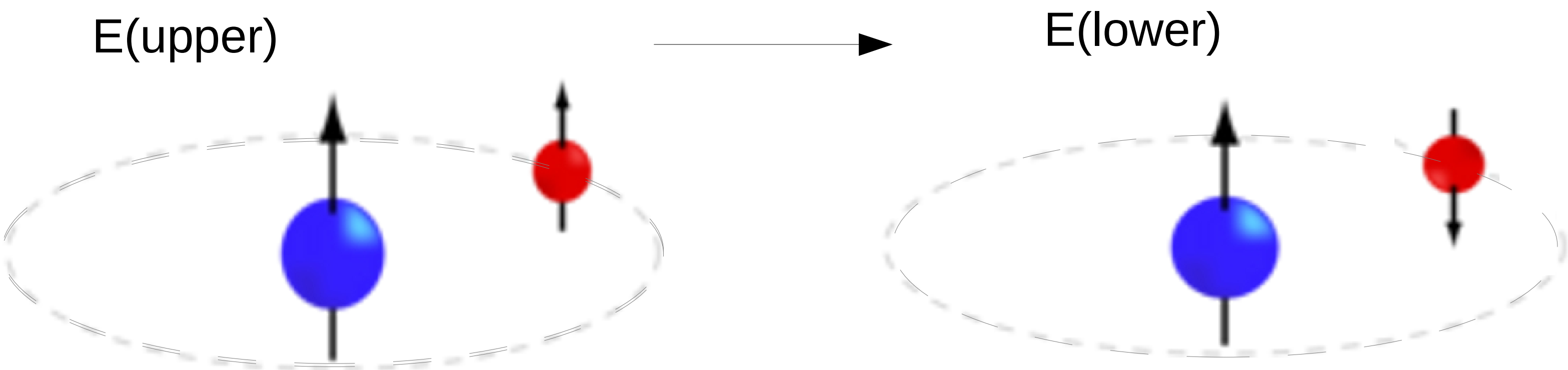

Transition is highly forbidden, with a probability of 2.9×10^{-15} s^{-1}; time for a single (isolated) atom to emit a 21.1 cm photon is $\sim 1.1 \times 10^{7}$ yrs. (Collisions reduce this time drastically...)

Transition is thus inefficient for cooling, and the temperature T_{spin} of the HI clouds is ~ 60-100K. HI clouds comprise ~10% of visible mass of a galaxy, but have typical densities $n_H \sim 1$ cm^{-3}, so they

- will never cool and collapse to form stars ($t_{ff} \sim 4 \times 10^{7}$ yrs)
- need to be compressed to form molecular hydrogen

Cool H_2 not easy to observe directly (I)

H_2 homonuclear so no permanent dipole moment. *Only (symmetric) quadrupole transitions permitted with $\Delta J = 0, +/- 2$*

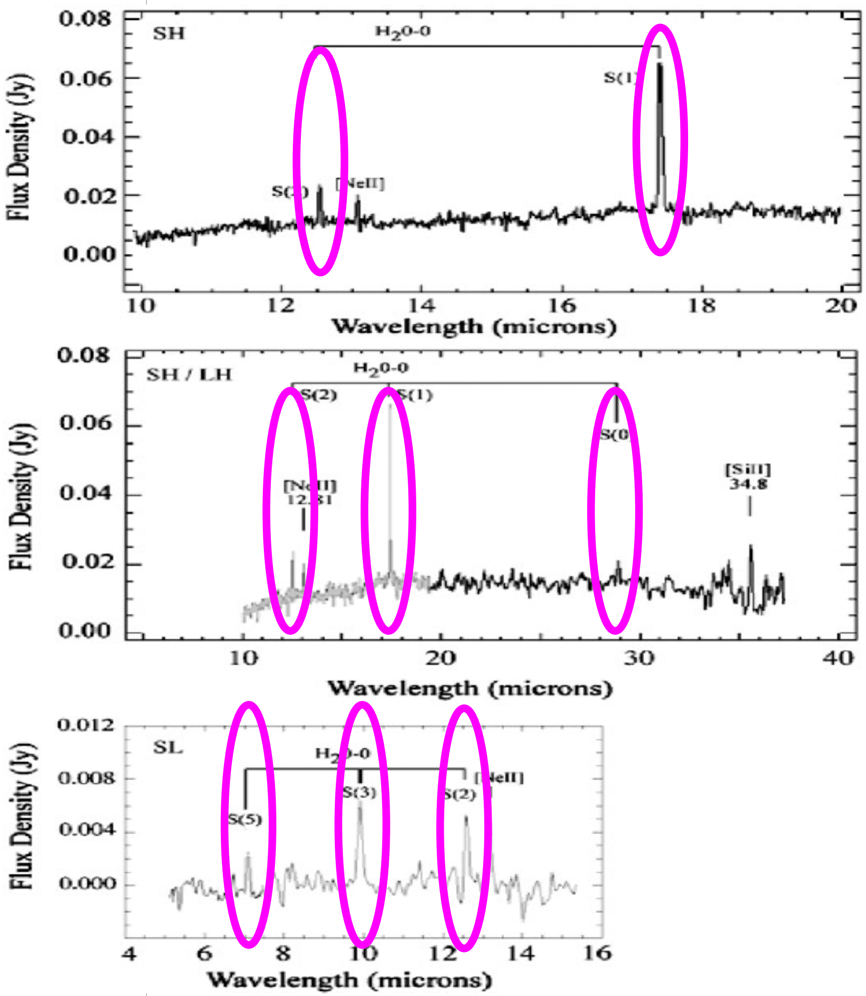

MIR emission lines: Vibrational ($\Delta V = 0$) transitions in the **mid-infrared** (5-28 μm).

Relatively low critical densities ($\geq 10^2$ - 10^3 cm^{-3}) so usually thermally excited, although beware of fluorescence and shocks

However, the warm molecular gas at these temperatures (100-1000K) is only a small fraction (~5%) of the cool molecular gas see Roussel et al. 2007).

Tip of the iceberg!

Spitzer IRS spectrum of brightest galaxy in Stephan's Quintet (Appleton+ 2006): shock excited!

Cool H_2 not easy to observe directly (II)

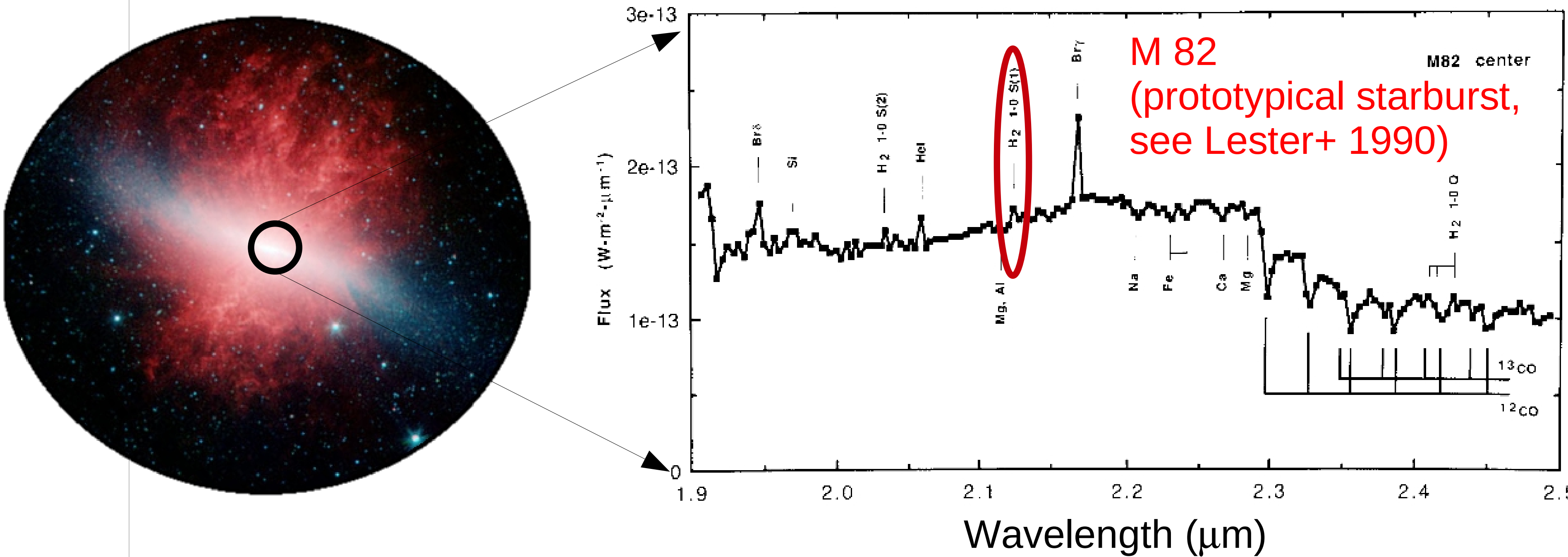

NIR emission lines: Roto-vibrational transitions in the **near-infrared** (1-2 µm). Critical densities are sufficiently high (> 10^4 cm^{-3}) that these transitions are usually *excited by fluorescence* (see Black & van Dishoeck 1987, Sternberg & Dalgarno 1989), rather than reflecting thermal equilibrium in the 1000-2000K regime.

AN EVEN SMALLER fraction (< 10^{-5}) of total cool molecular gas (see Dale et al. 2005)

Cool H_2 *in* *dusty* *regions is virtually impossible*

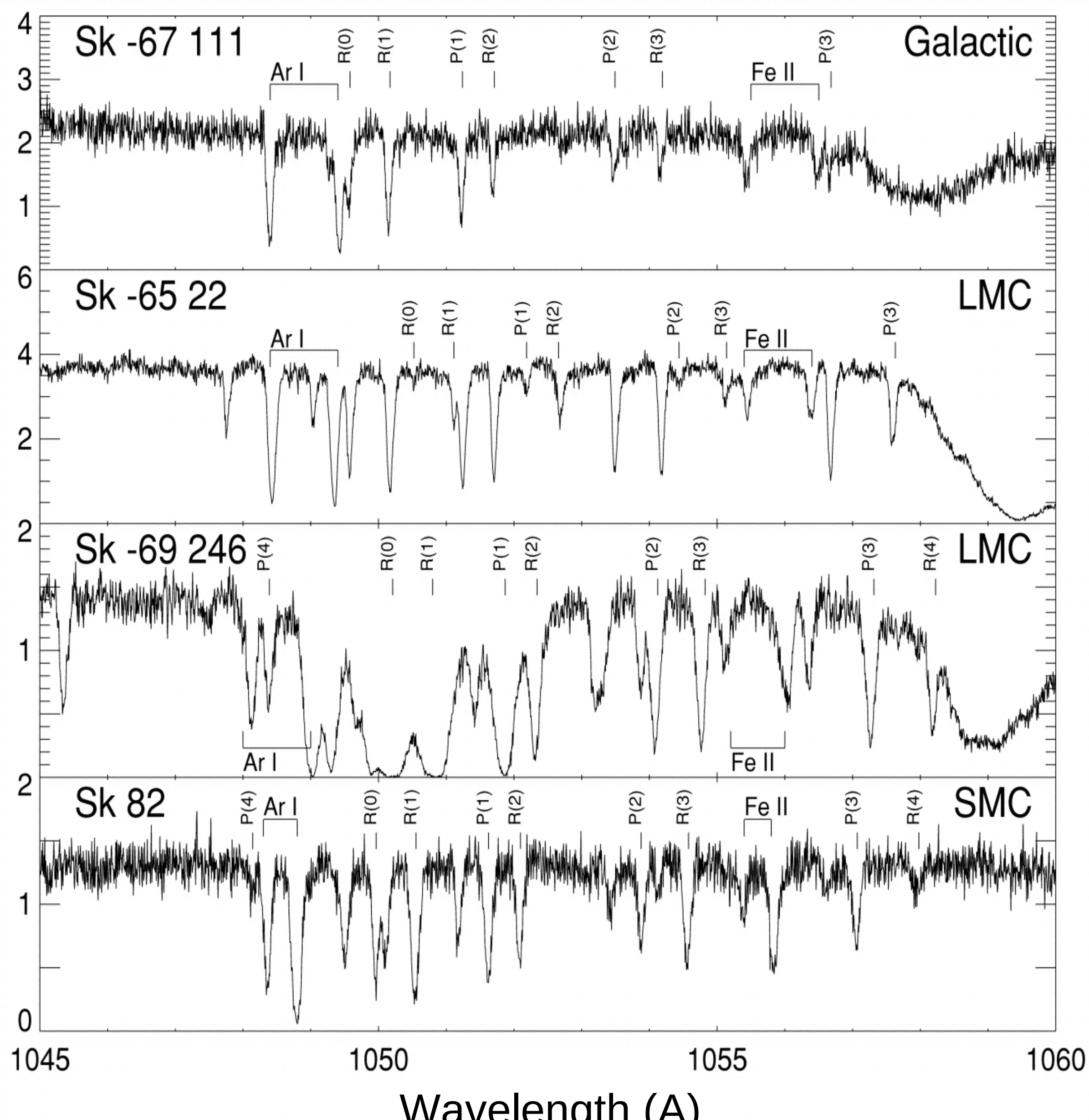

FUV (usually) absorption lines:

Electronic transitions in the **far-ultraviolet** (absorption of a Lyman-Werner photon with energies 11.2-13.6 eV, i.e. the origin of *fluorescence*, see Sternberg 1989).

~10-15% of these absorptions result in dissociation of the molecule.

But need a dust-free sightline (AV ≤ 1) in front of a bright star, so virtually impossible to detect them in dusty regions (see FUSE results, e.g., LMC/SMC: Tumlinson+ 2002).

CO to the rescue...

- ^{12}CO is the most abundant molecule after H_2:
  $N(CO)/N(H_2) \sim$ few $\times 10^{-5}$ to 10^{-4}

- Permanent dipole moment →
  Dipole transitions allowed with $\Delta J = +/-1$

- Small dipole moment $\mu_{el} \sim 0.1$ Debye →
  Rotational transitions visible at sub-mm, mm wavelengths
  Collisions can populate lowest levels even at low densities

- Excited by UV radiation field and collisions with H_2, but too much radiation (from 11.1 to 13.6 eV) causes CO to dissociate, so need self-shielding (protection from the radiation field)

- Must reside in cold (10-40K) dense ($\geq 10^3$ cm^{-3}) clouds

X factor: Relating CO luminosity to H_2 mass

CO emission is optically thick (e.g., Wilson+ 1974), hence traces surface area, not volume ➜ need proportionality constant X to relate Intensity(CO) to mass or column density, N_{H2}

Assumptions (e.g., Dickman+ 1986):

(1) Extragalactic molecular emission distributed as an ensemble of independent discrete clouds (no overlap along LOS)

(2) Individual clouds virialized (line width $\leftrightarrow$ dynamical mass)

virialization

mass in homogeneous sphere

$$I(CO) = \int T_b\, dv \cong \sum T_b \Delta v \sim \sum T_b\, (M/r)^{1/2} \sim T_b \sum (n_{H2})^{1/2}\, r$$

$N_{H2} = (n_{H2})\, r$

$$\sim \left[T_b\, (n_{H2})^{-1/2}\right] N_{H2}$$

Hence, $N_{H2} = X \times I(CO)$, where $X \sim (n_{H2})^{1/2} / T_b$

Empirically, $X = 2\text{-}5 \times 10^{20}\ \mathrm{cm^{-2}\ K^{-1}\ km^{-1}\ s}$

Circumnuclear regions: where the action is

Galactic nuclei characterized by high (stellar) mass concentration

- *bulges, pseudobulges, stellar bars*
- *massive star clusters, nuclear disks, cusps, cores, ...*

Molecular gas (not atomic) also tends to pile up in the central kpc of galactic nuclei

- *nuclear gas disks, rings, bars and spirals*

Why does the gas gravitate toward the circumnuclear regions?

- *deeper gravitational potential*
- *tidal interactions and mergers rearrange gas and drive gas inflow*
- *secular evolution driven by bars and spiral structure density waves acting on disk material*

Local deviations from exponential disk

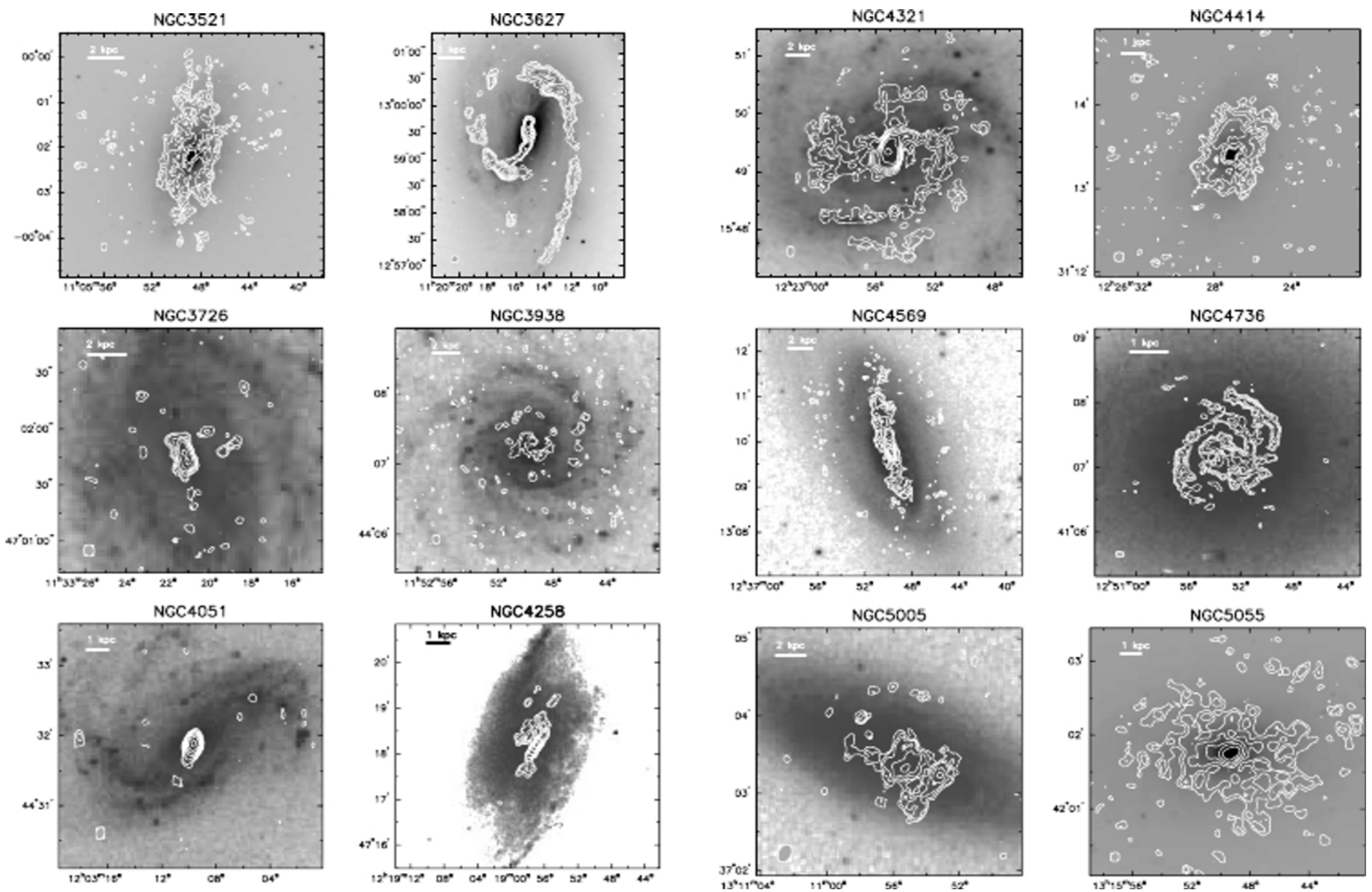

On kpc circumnuclear spatial scales, there are deviations from the exponential stellar disk: rings, holes, spirals, bars, ... (see BIMA-SONG survey, Helfer+ 2001, 2003).

Interferometric CO surveys of galaxies

Project	N	Line	Telescope	Aim	
BIMA-SONG, Helfer et al.	44	CO(1-0),	BIMA,	CO properties normal	***6”***
OVRO-NMA, Sakamoto et al. 1999	20	CO(1-0)	OVRO, NRT	Barred vs non-barred	***4”***
SCONES, Petitpas et al. 2006	~10	CO(2-1), CO(3-2)	SMA	Warm gas properties normal galaxies	***1-3”***
NUGA, Garcia-Burillo, Combes et al.	25	CO(1-0), CO(2-1)	PdBI	Gas and Nuclear activity	***0.5-1”***
Seyfert, Matsushita, Kohno et al.	~10	CO(1-0), CO(2-1),CO(3-2) , HCN, HCO+	NRT, SMA	Gas and Nuclear activity	***4”***
LIRGs/ULIRGs, Wilson et al. 2008, Iono et al. 2009	11	CO(2-1), CO(3-2)	SMA	Physical properties gas in merger systems	***1-3”***

To probe critical scales for AGN fueling (10-100pc), high-spatial resolution is key!

(taken from S. Garcia-Burillo)

Interferometric CO surveys of galaxies

Project	N	Line	Telescope	Aim	
BIMA-SONG, Helfer et al.	44	CO(1-0),	BIMA,	CO properties normal	***6”***
OVRO-NMA, Sakamoto et al. 1999	20	CO(1-0)	OVRO, NRT	Barred vs non-barred	***4”***
SCONES, Petitpas et al. 2006	~10	CO(2-1), CO(3-2)	SMA	Warm gas properties normal galaxies	***1-3”***
NUGA, Garcia-Burillo, Combes et al.	25	CO(1-0), CO(2-1)	PdBI	Gas and Nuclear activity	***0.5-1”***
Seyfert, Matsushita, Kohno et al.	~10	CO(1-0), CO(2-1),CO(3-2) , HCN, HCO+	NRT, SMA	Gas and Nuclear activity	***4”***
LIRGs/ULIRGs, Wilson et al. 2008, Iono et al. 2009	11	CO(2-1), CO(3-2)	SMA	Physical properties gas in merger systems	***1-3”***

To probe critical scales for AGN fueling (10-100pc), high-spatial resolution is key!

(taken from S. Garcia-Burillo)

The NUGA survey at IRAM-Plateau de Bure

S. Garcia-Burillo, F. Combes, A. Baker, F. Boone, A. Eckart, P.Englmaier, L. Hunt, S. Leon, R. Neri, E. Schinnerer, L. Tacconi + M. Krips, V. Casasola

- 200 hrs observing time at PdBI, in ABCD configurations, over about 3 yrs (2001-2003). ^{12}CO(1-0) 115.27 GHz, ^{12}CO(2-1) 230.54 GHz

- Spatial resolution ~0.6" (at 230 GHz) – 2" (worst case 115 GHz). PdBI primary beam size 42" (115GHz), 21" (230GHz). Velocity resolution 10 km/s; continuum sensitivity ~ 2 mJy/beam (115 GHz), ~5 mJy/beam (230 GHz).

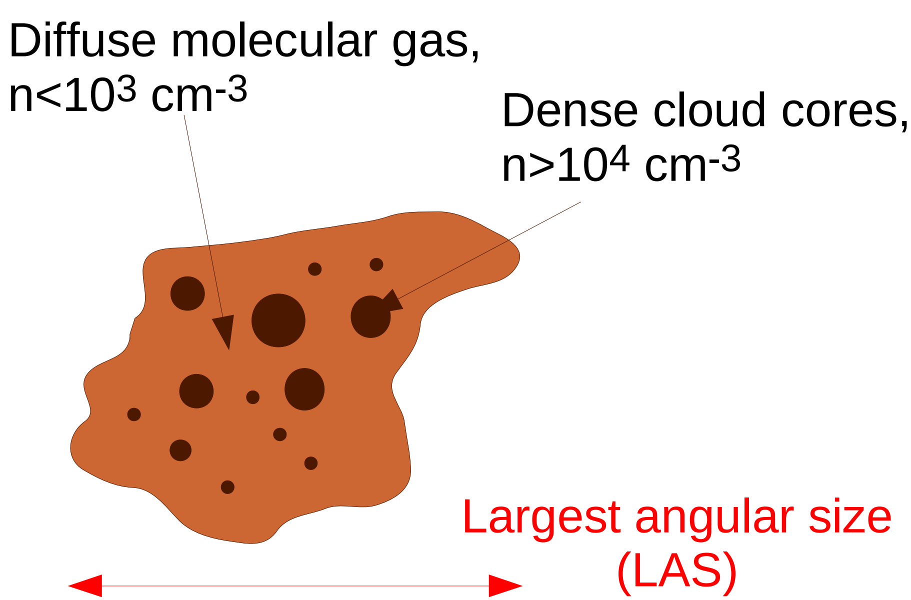

Subsequent 30-meter single dish (Pico Veleta) observations for short-spacing correction to ***recover diffuse flux possibly resolved out by interferometric observations:*** half-power beam size 22" (115 GHz), 12" (230 GHz)

NUGA CO images of galaxies (Papers I-XIV)

(Garcia-Burillo+ 2003, 2005, 2009; Combes+ 2004, 2009; Krips+ 2005, 2006, 2007; Boone+ 2007; Lindt-Krieg+ 2008; Hunt+ 2008; Casasola+ 2008, 2009; van der Laan+ 2010)

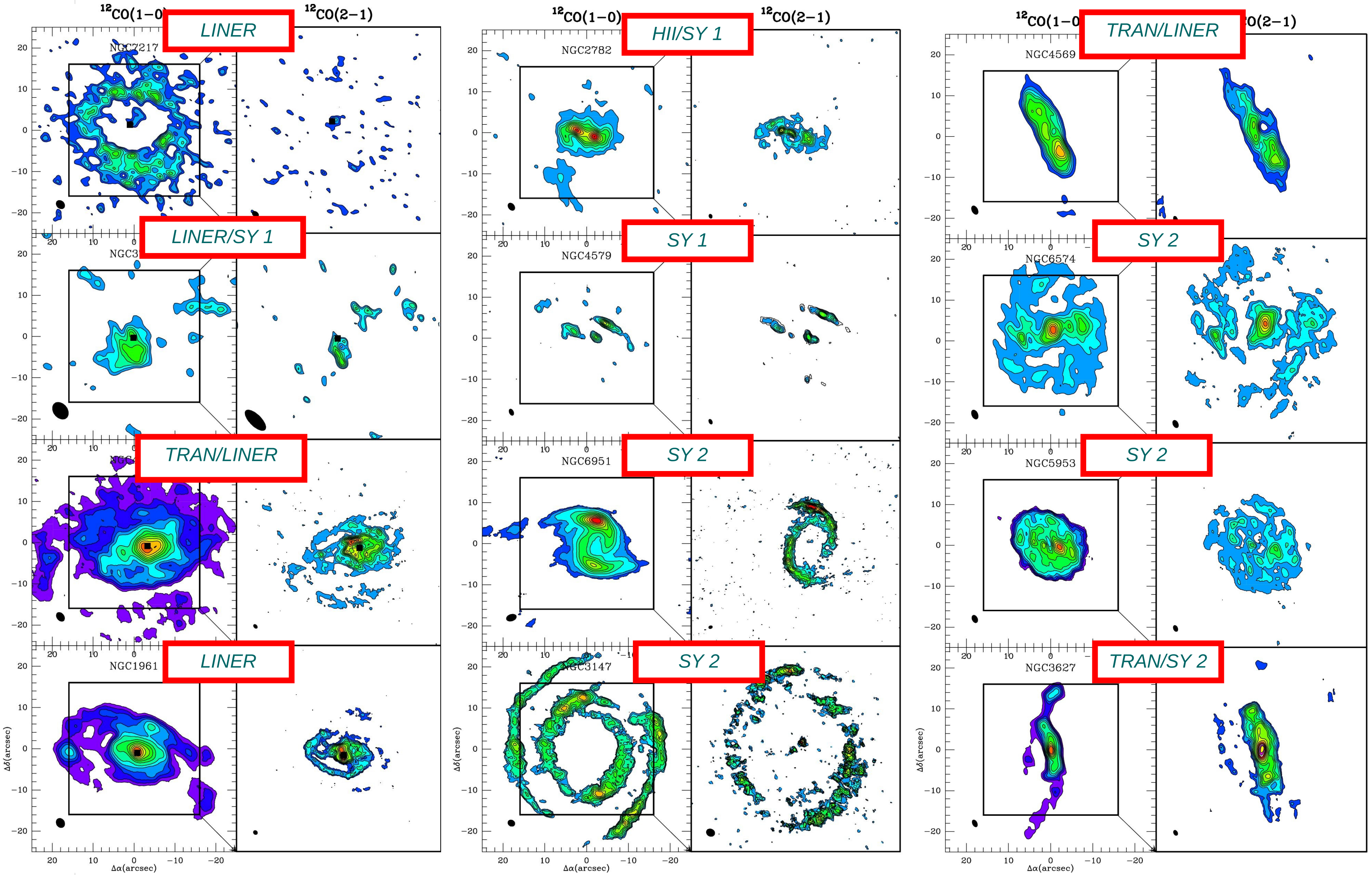

NUGA CO images of galaxies (Papers I-XIV)

(Garcia-Burillo+ 2003, 2005, 2009; Combes+ 2004, 2009; Krips+ 2005, 2006, 2007; Boone+ 2007; Lindt-Krieg+ 2008; Hunt+ 2008; Casasola+ 2008, 2009; van der Laan+ 2010)

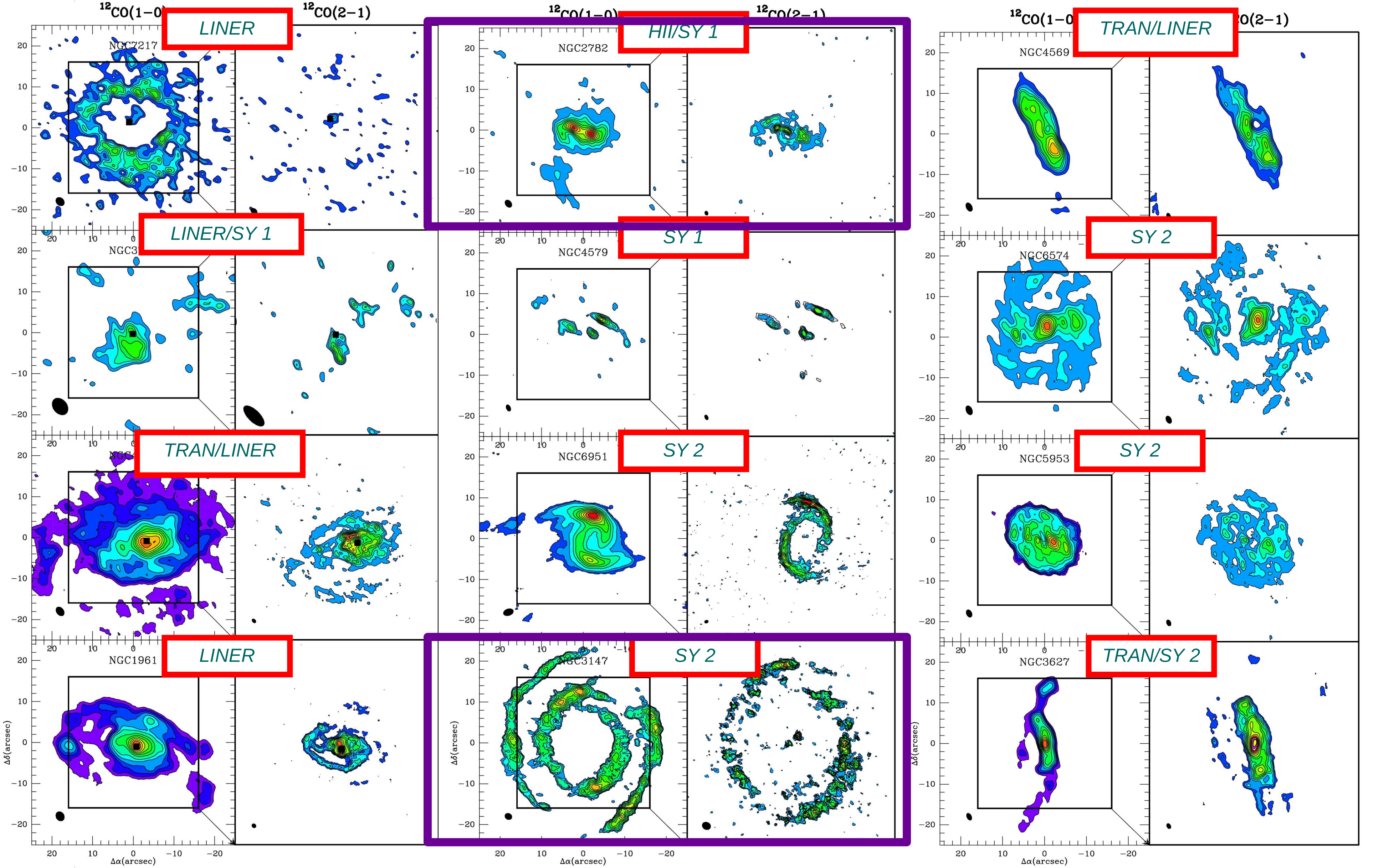

NUGA IX. NGC 2782

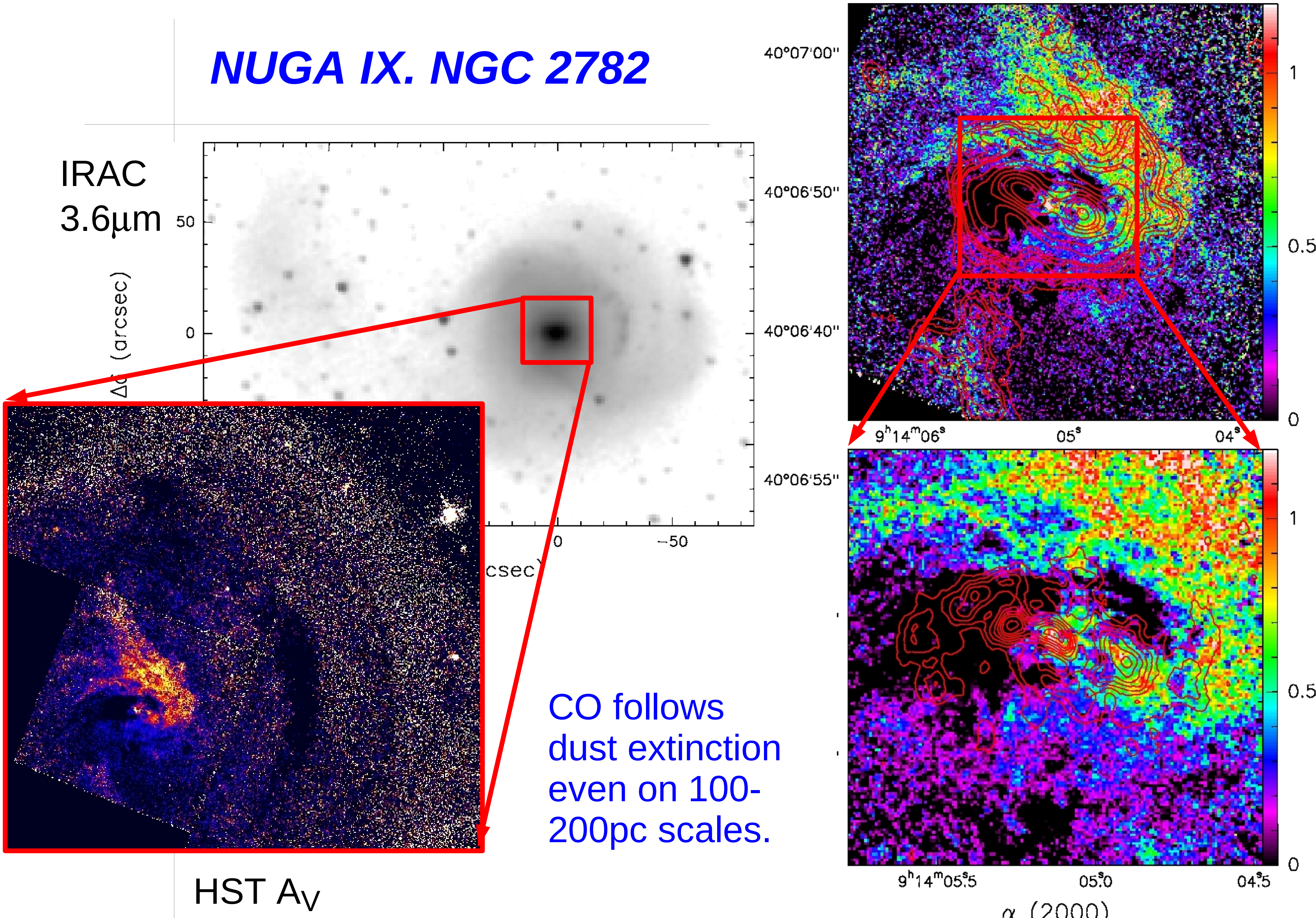

CO follows dust extinction even on 100-200pc scales.

NGC 2782: contrasting spatial scales for HI, CO

HI plume on 50-60 kpc scales to northwest (Smith 1991)

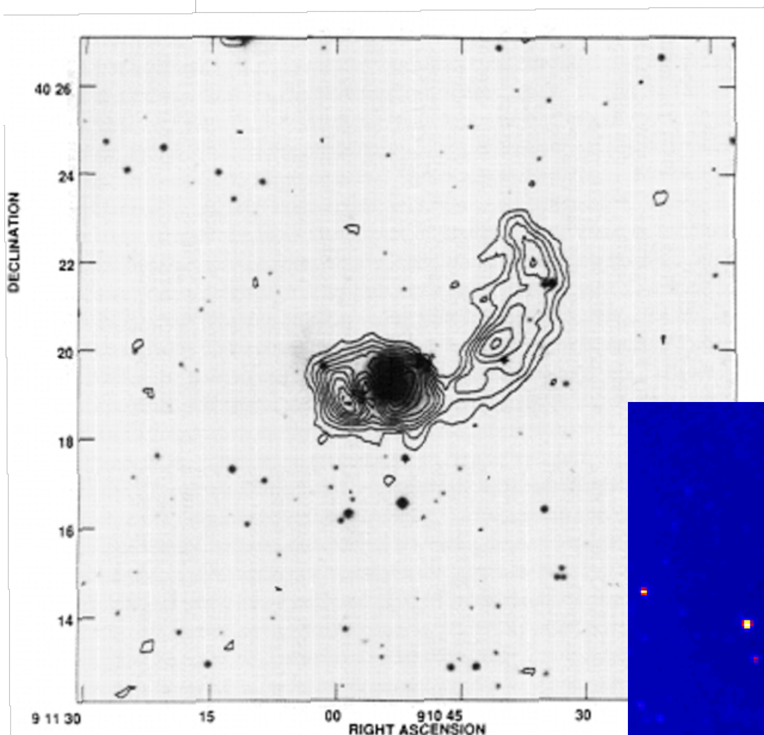

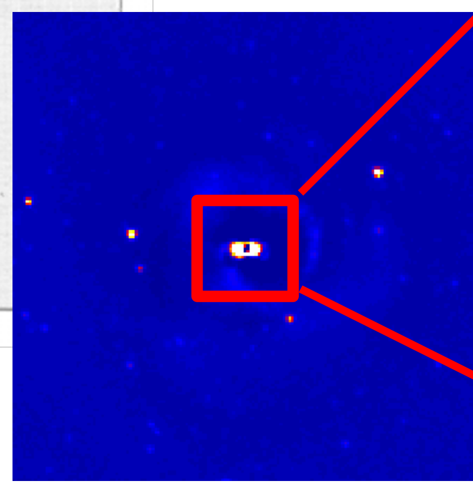

3.6 µm bulge-disk residuals

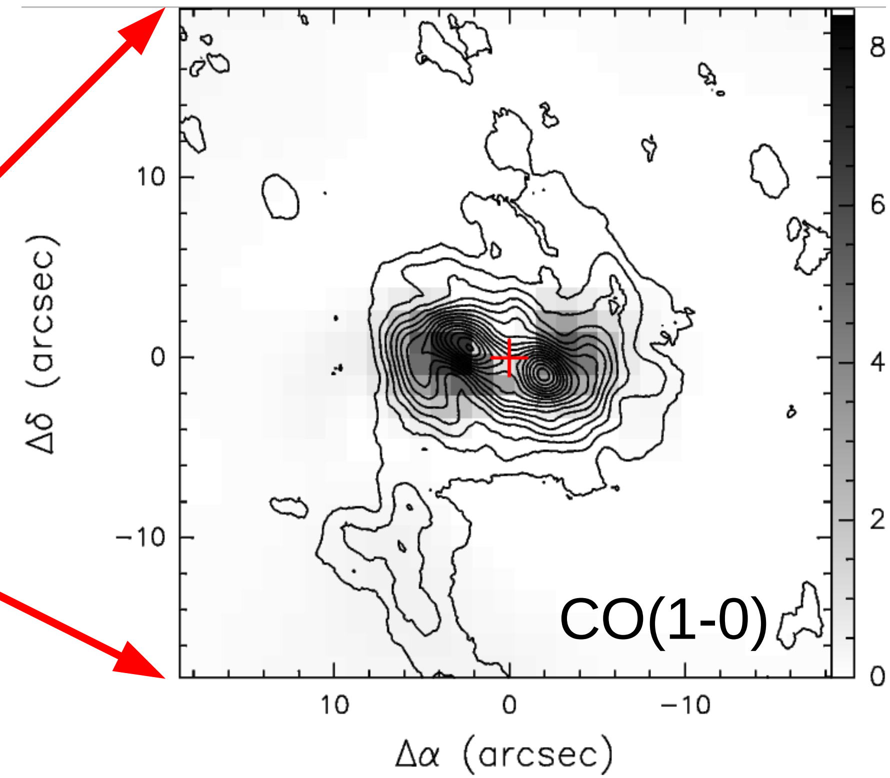

Bulge-disk decomposition subtracted from 3.6 µm image (Hunt+ 2008) shows stellar bar, diameter ~ 700pc

NGC 2782: contrasting spatial scales for HI, CO

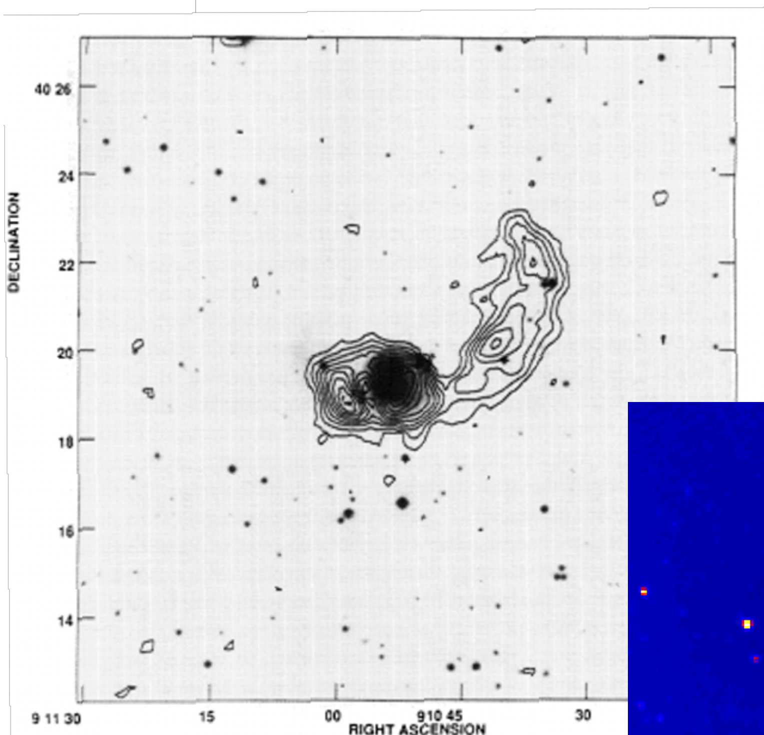

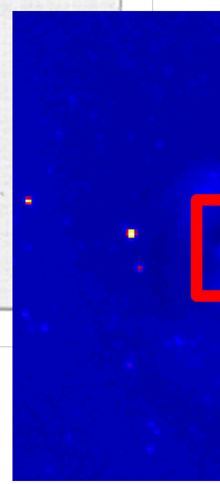

HI plume on 50-60 kpc scales to northwest (Smith 1991)

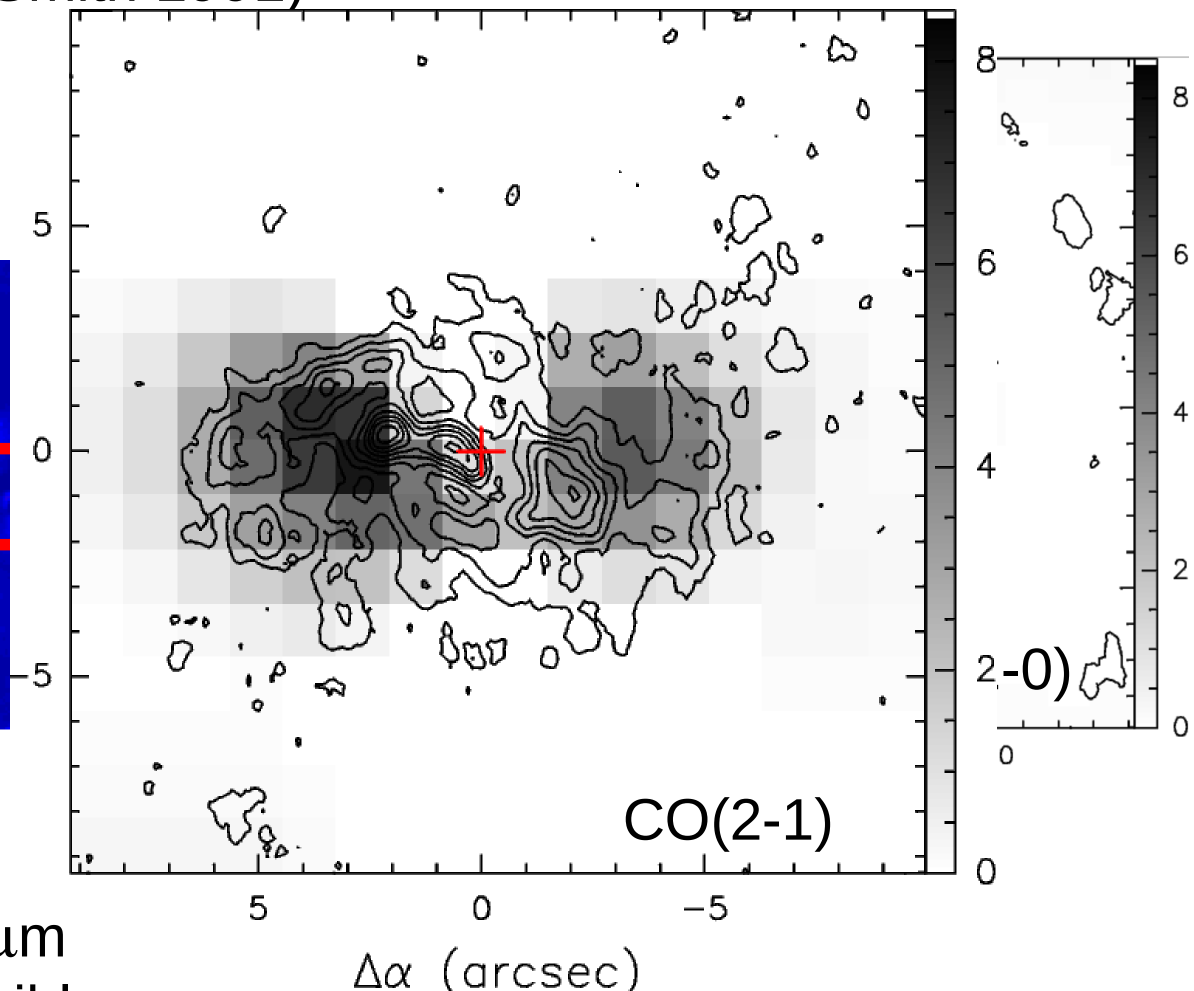

Nuclear molecular bar aligns perfectly with stellar bar seen in 3.6 µm residuals (not easily visible without subraction)

NUGA X. NGC 3147

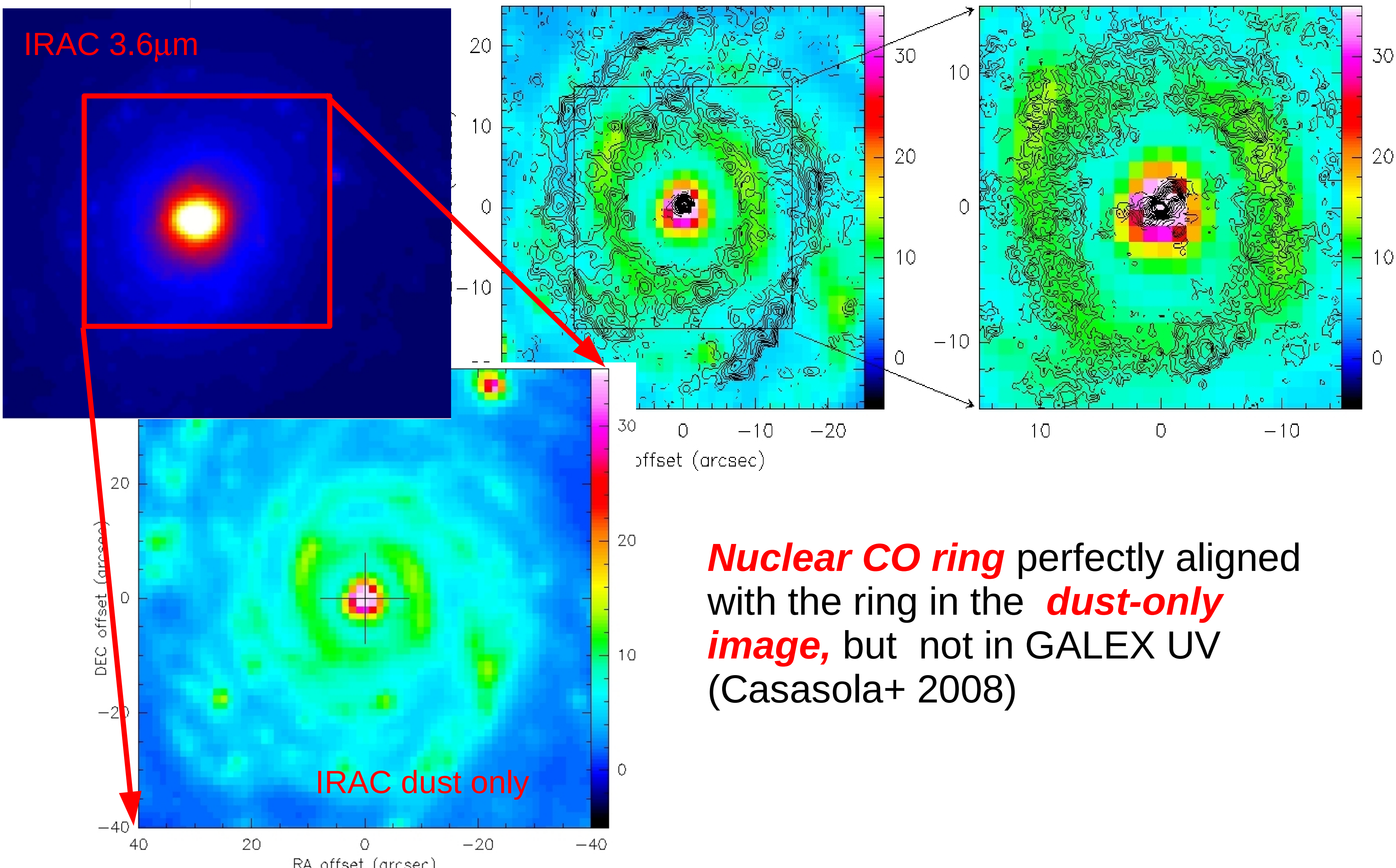

Nuclear CO ring perfectly aligned with the ring in the ***dust-only image,*** but not in GALEX UV (Casasola+ 2008)

CO circumnuclear morphology: a mixed bag

- H_2 masses in the inner kpc region range from: 3 - 5 $\times 10^8$ to $> 10^9$ Msun. The extraordinary case of NGC 1961 (Combes+ 2009) has $M(H_2) \sim 2 \times 10^{10}$ Msun.

- $M(dyn) \sim RV^2/G$. $M(H_2)/M(dyn)$ from a few percent up to > 20%. *This means that more than 1/5 of the mass in the central few kpc of a galaxy can be molecular gas!*

- There is *no unique morphology* associated with central regions of galaxies hosting low-luminosity active galactic nuclei (AGN). NUGA finds *gas rings, nuclear gas bars, nuclear spiral arms, disks, and lopsidedness,* which may or may not be associated with stellar features (or with gas inflow to the AGN).

- *CO generally follows the **dust** distribution*, but with some very local (scales > 300 pc) variations... *Multiwavelength analysis important!*

Gas surface density correlated with star formation

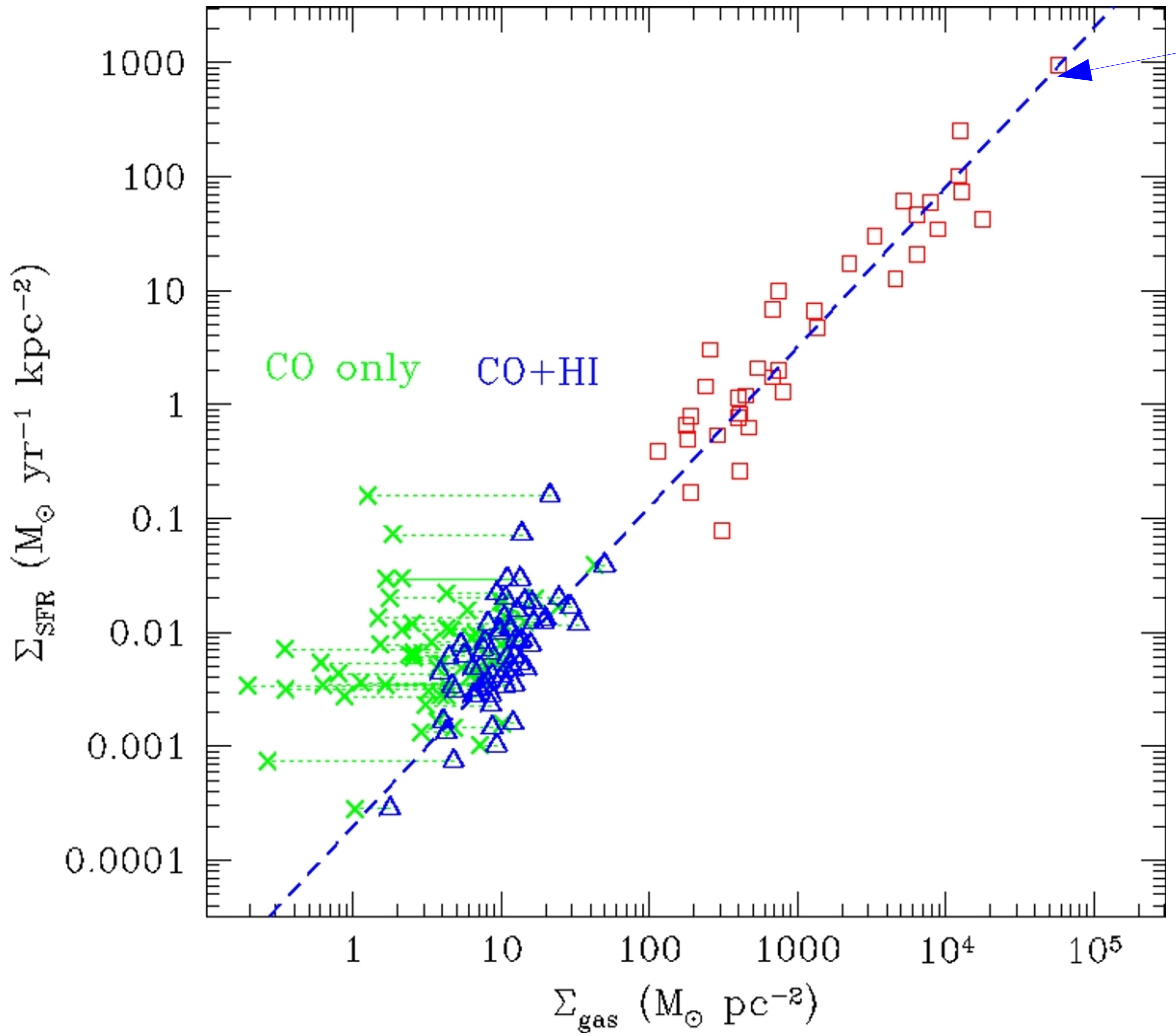

slope = 1.4

Circumnuclear starbursts, ultraluminous infrared galaxies need only H_2 (CO).

Most normal spirals need H_2+HI to bring them onto correlation!

***Global** Kennicutt-Schmidt law: discovered by Schmidt (1959) for HI. Extended to total gas H_2+HI by Kennicutt (1989,1998).*

The spatially resolved Kennicutt-Schmidt law

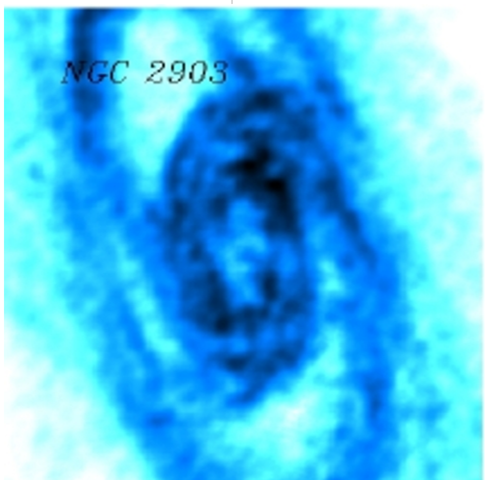

+

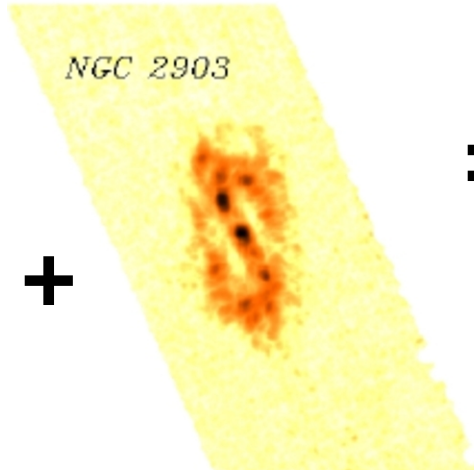

HI **CO**

= Total gas density, Σ_{gas}

High-resolution **HI** and **CO** maps
(THINGS: Walter et al. 2008;
HERACLES: Leroy et al. 2009)

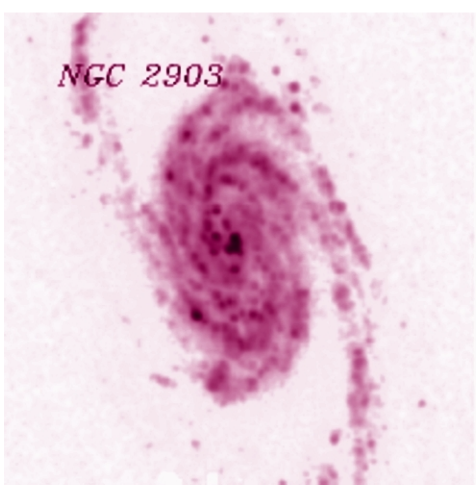

+

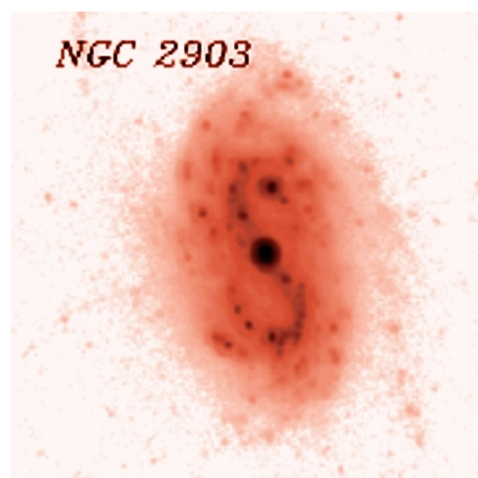

FUV **24 µm**

= Total star formation rate, Σ_{SFR}

SFR from **GALEX FUV** + **Spitzer 24 µm** (Bigiel et al. 2008)

Star formation and H_2

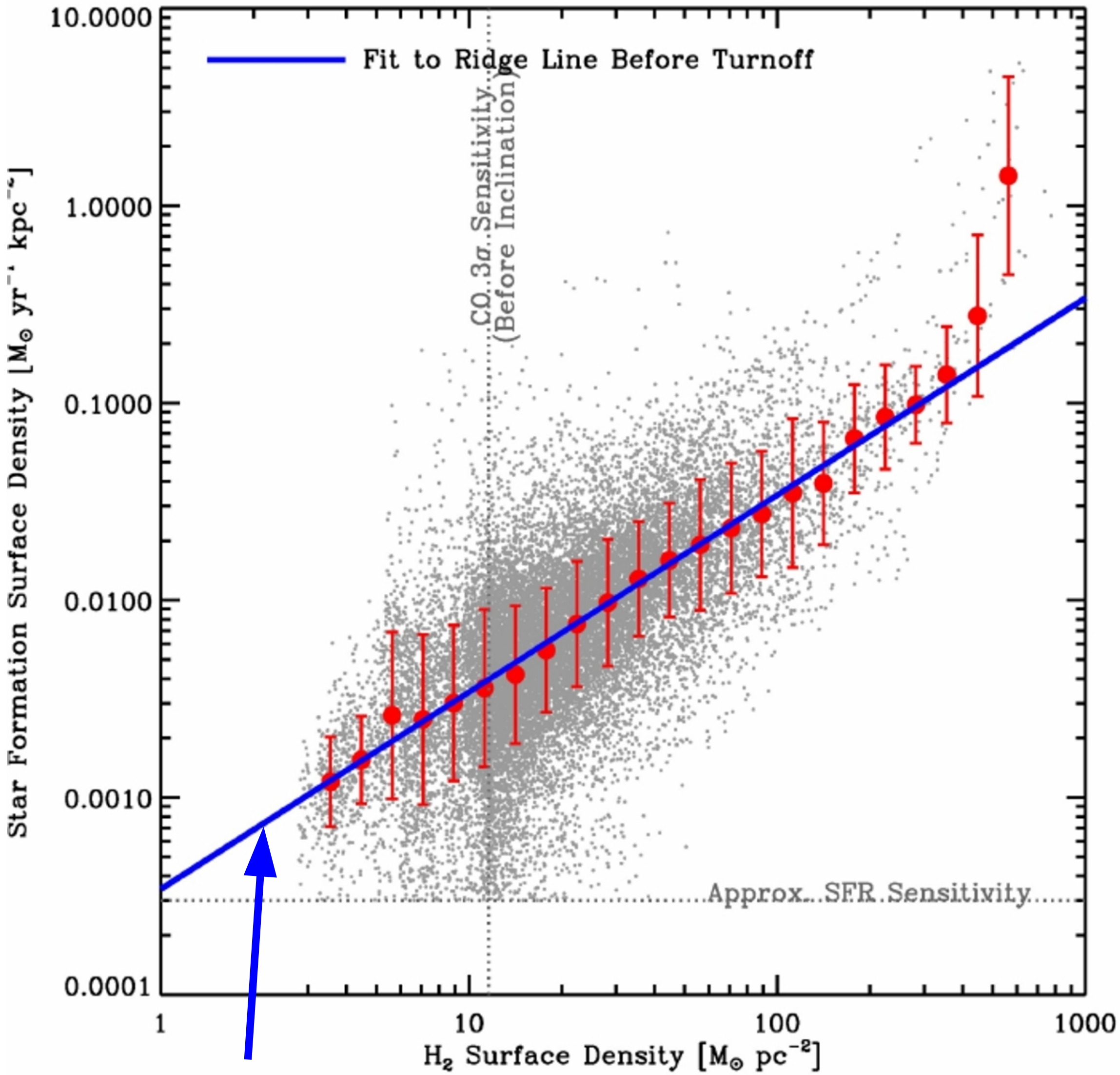

slope = 1.0 +/- 0.2

Gray points:
- ✔ individual data, pixel-by-pixel, from 23 galaxies
- ✔ 13" resolution, Nyquist sampled
- ✔ 30000 independent measurements

Red points:
- ✔ Median and scatter of binned data

(Leroy et al. 2008, 2009)

Star formation and HI

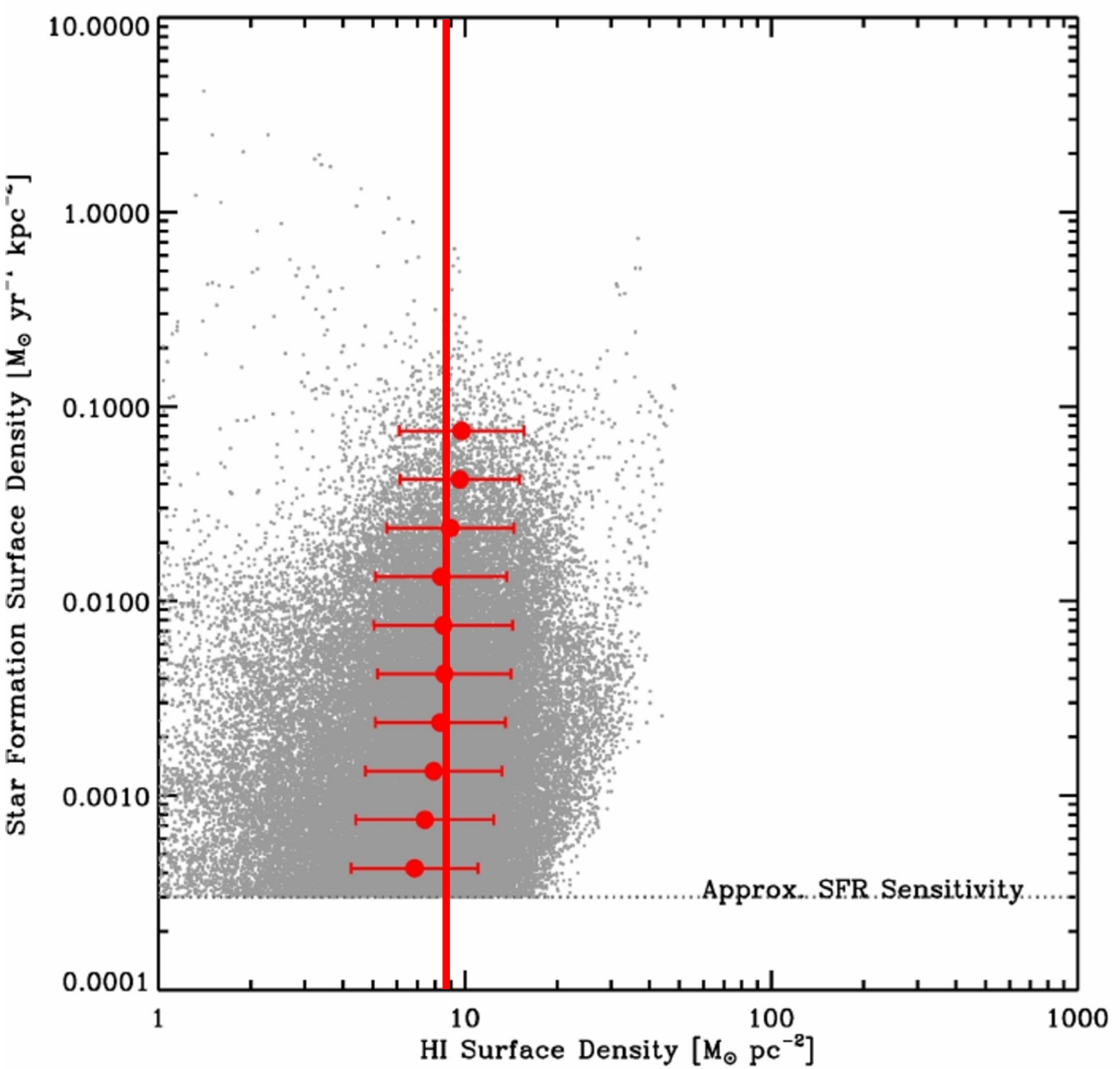

Gray points:
- ✔ individual data, pixel-by-pixel, from 23 galaxies
- ✔ 13” resolution, Nyquist sampled
- ✔ 30000 independent measurements

Red points:
- ✔ Median and scatter of binned data

(Leroy et al. 2008, 2009)

Σ_{HI} “saturates” at ~ 9-10 M_{sun} pc^{-2} and is not correlated with Σ_{SFR}

Where do stars form?

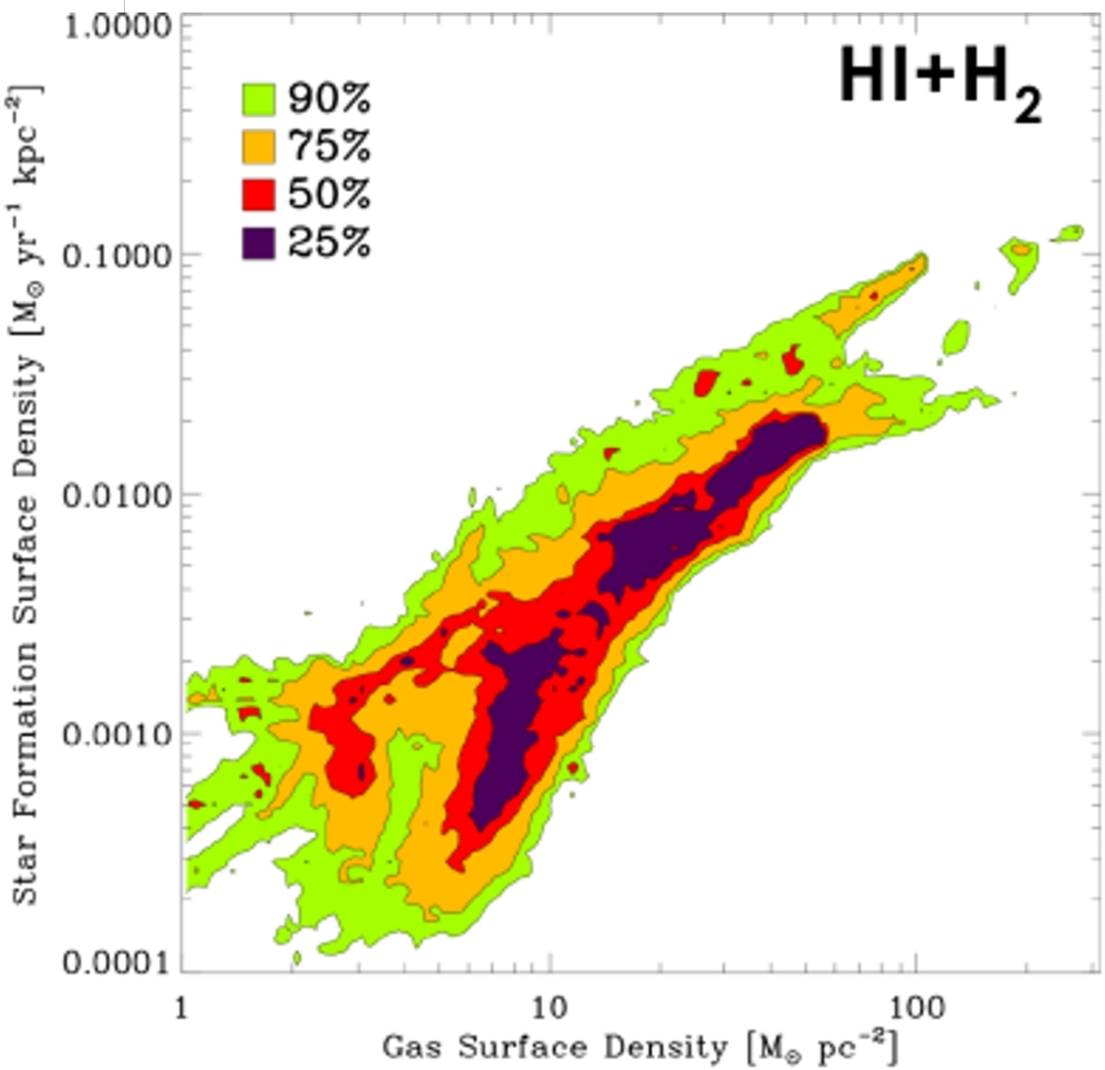

Contours reflect data density of points averaged over ensemble of galaxies; equal weight to each radius (taken from Bigiel et al. 2008, Leroy et al. 2008, 2009).

- *Σ_{HI} saturates at ~ 9-10 Msun pc^{-2}*
- *Σ_{H2} correlates with Σ_{SFR} (slope = 1.0 +/- 0.2).* ***Stars form where molecular gas is dense.***
- *Molecular gas KS law, but hot debate! (see Krumholz+ 2008, 2009 for theoretical motivation)*

II. CO kinematics in galaxies

Velocity moments and CO data cubes

Channel map: 1 channel = 10 km/s

velocity -240 km/s

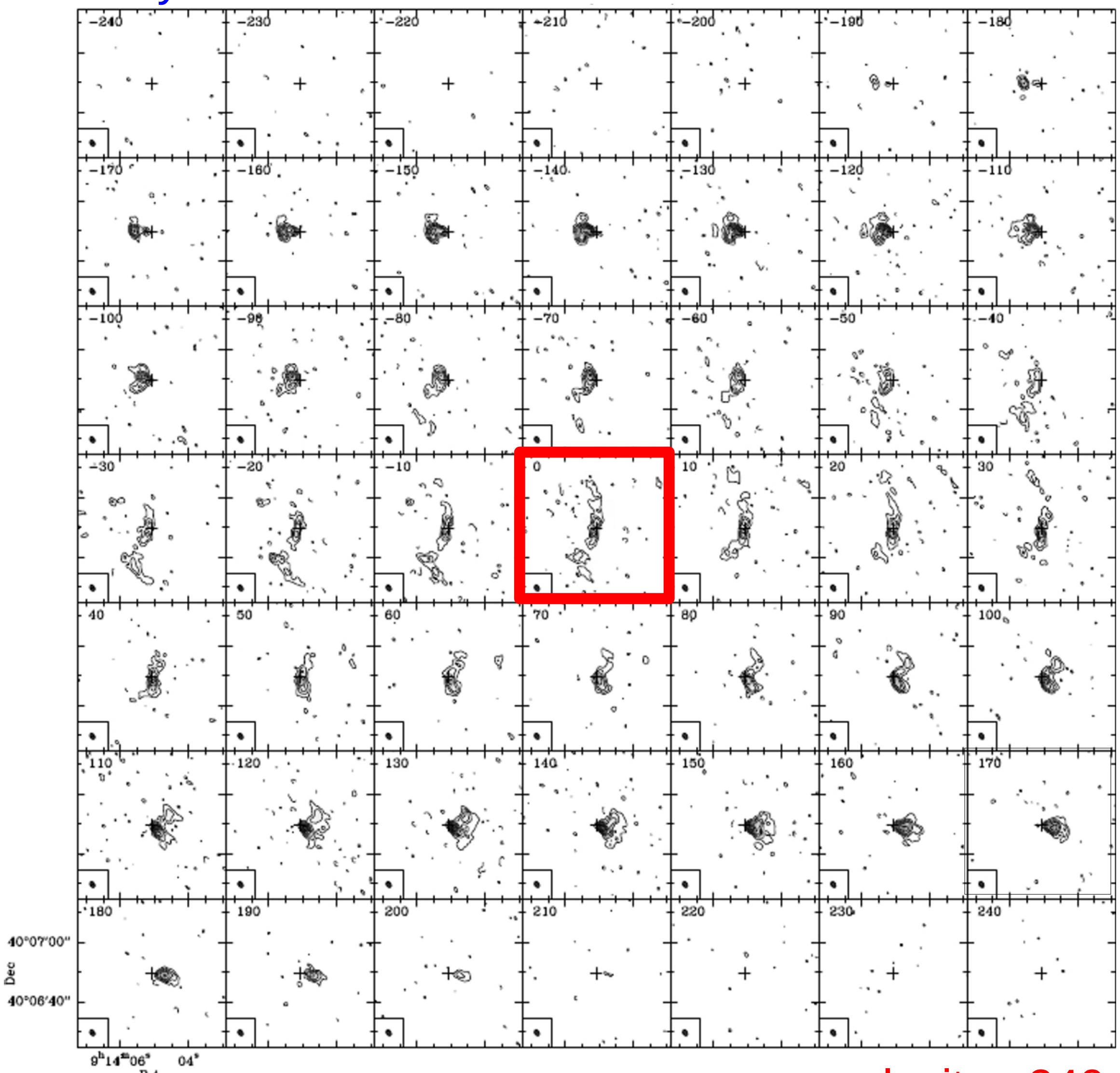

velocity +240 km/s

Position

Intensity maps =
zeroth-order moment =
$I(CO) = \int T_b \, dv$

Velocity field maps =
first-order moment =
$\int T_b \, v \, dv$

Intensity-weighted velocities;
if optically thin line, then would be mass weighted.

Iso-velocity ("spider") diagrams

But do NOT forget CO is optically thick

Disk must be inclined to line of sight

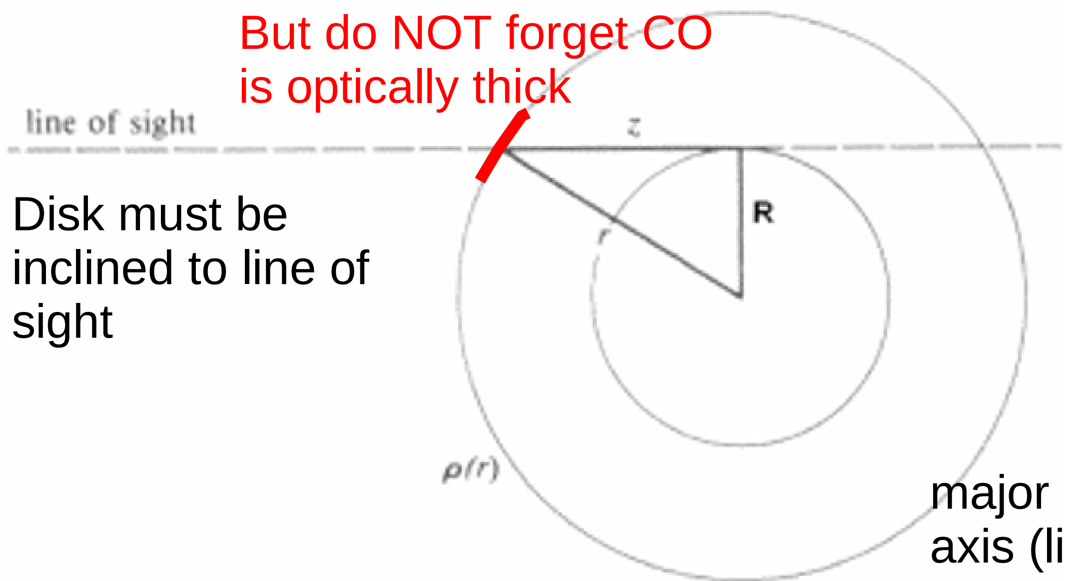

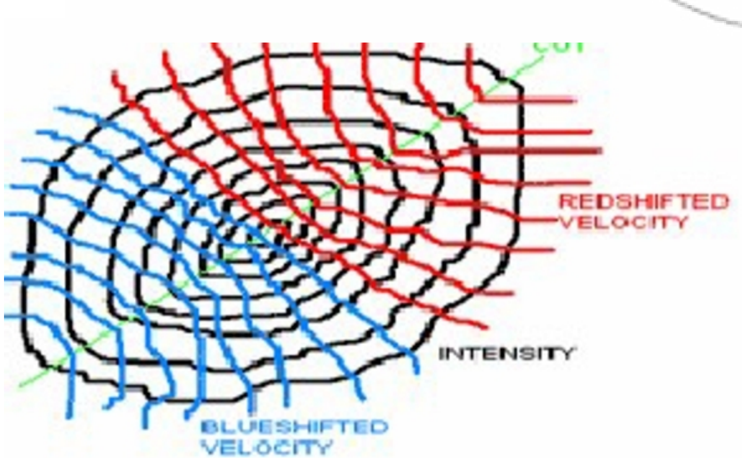

Schematic of iso-velocity contours superposed on intensity contour map

major axis (line of nodes)

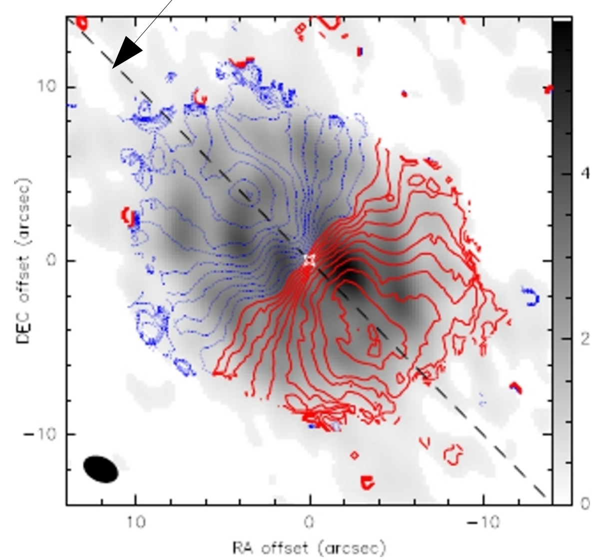

NGC 5953 (Casasola+ 2009)

nuclear gas bar

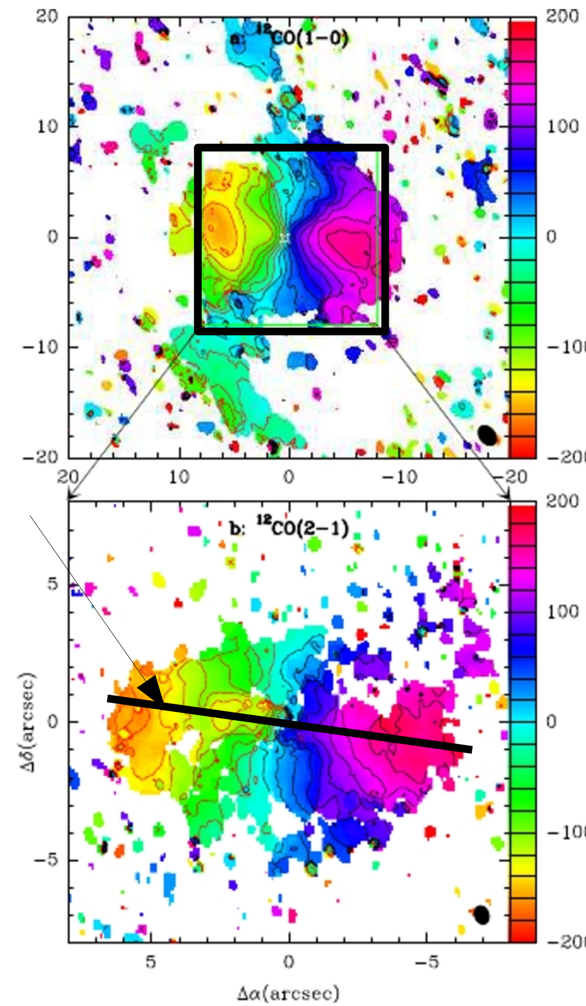

NGC 2782 (Hunt+ 2008)

Cuts along the major and minor axes...

major axis (line of nodes)

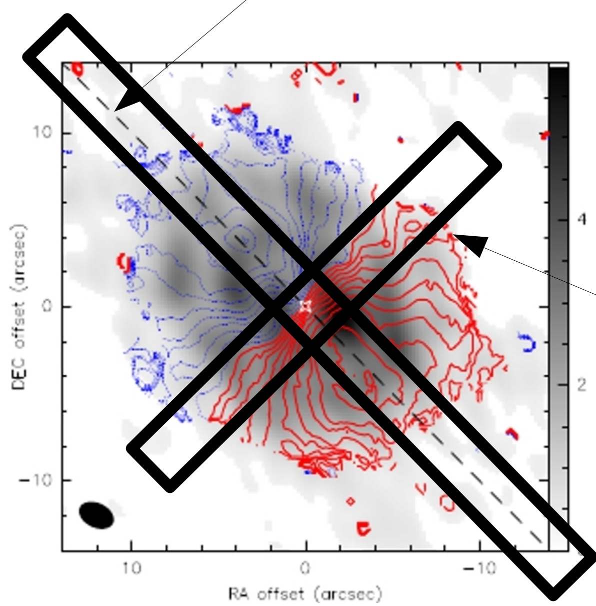

minor axis (rotation axis)

NGC 5953

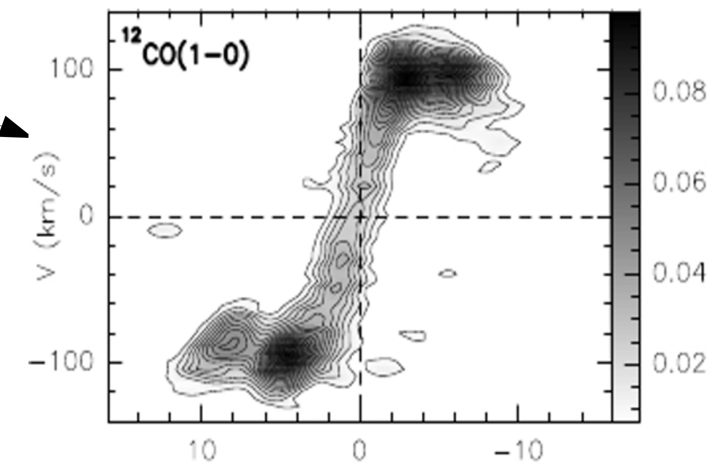

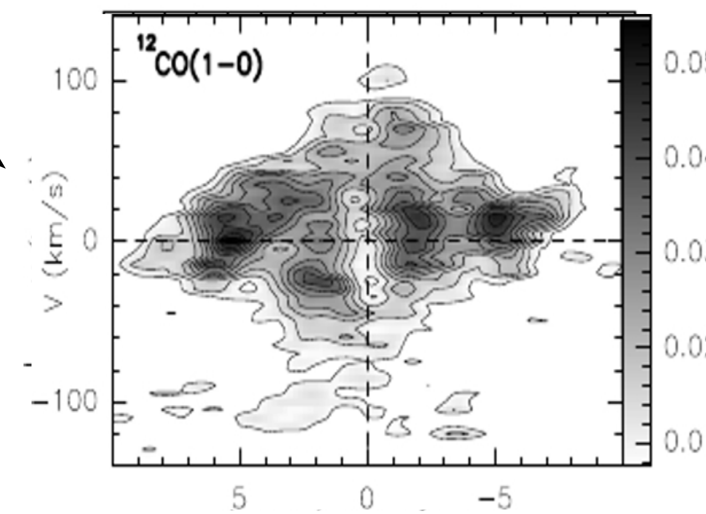

Distance in arcsec along major (top) minor (bottom)

... give position-velocity diagrams (Casasola+ 2009)

Position-velocity (PV) diagrams

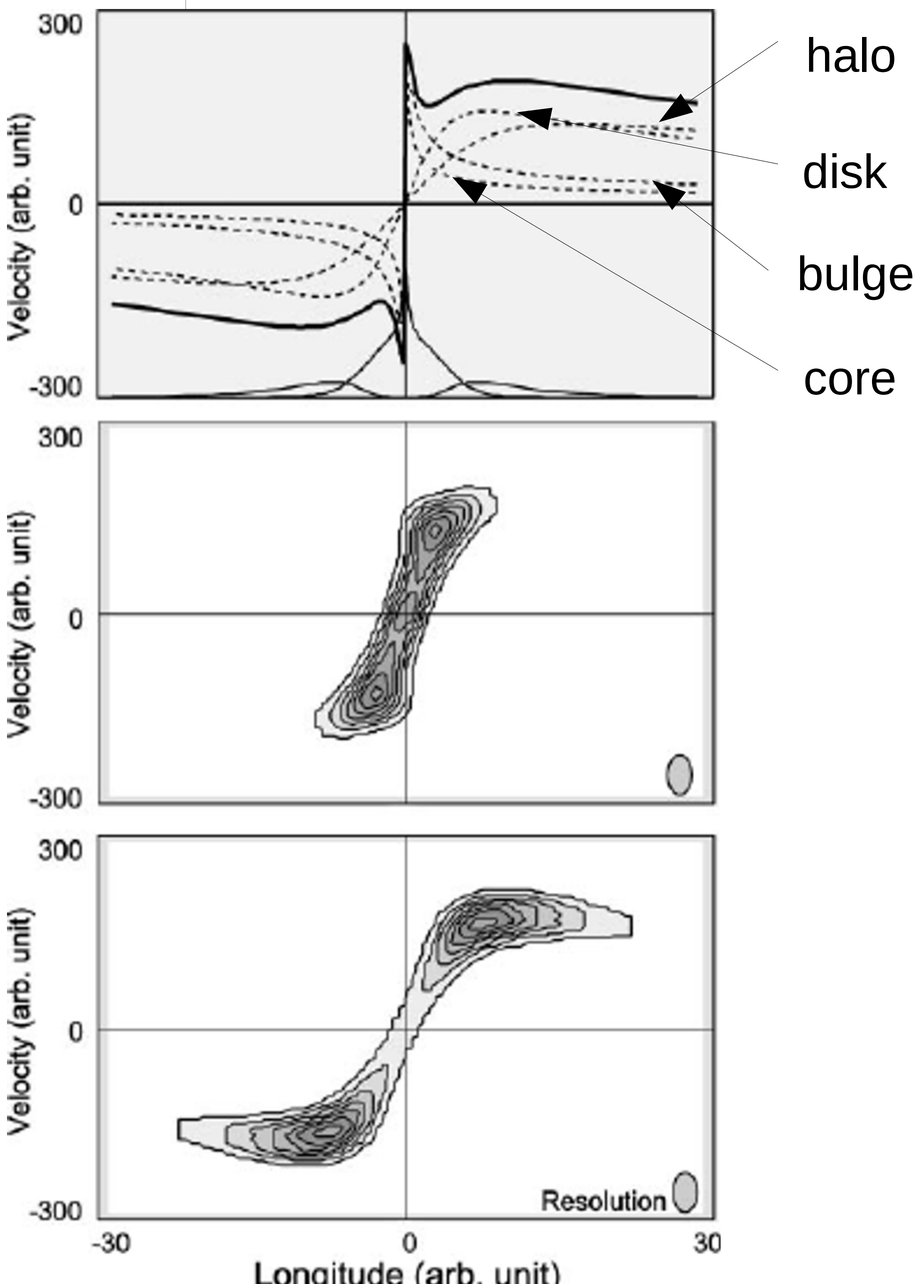

Simulations of beam-smearing on a major-axis PV diagram.

Top: Assumed "true" rotation curve (thick) with a central core, bulge, disk, and halo

Middle: "Observed" CO PV diagram

Bottom: "Observed" HI PV diagram

High resolution + high sensitivity necessary to detect central high velocities and steep rise

(taken from Sofue & Rubin 2001)

Observed major-axis PV diagrams

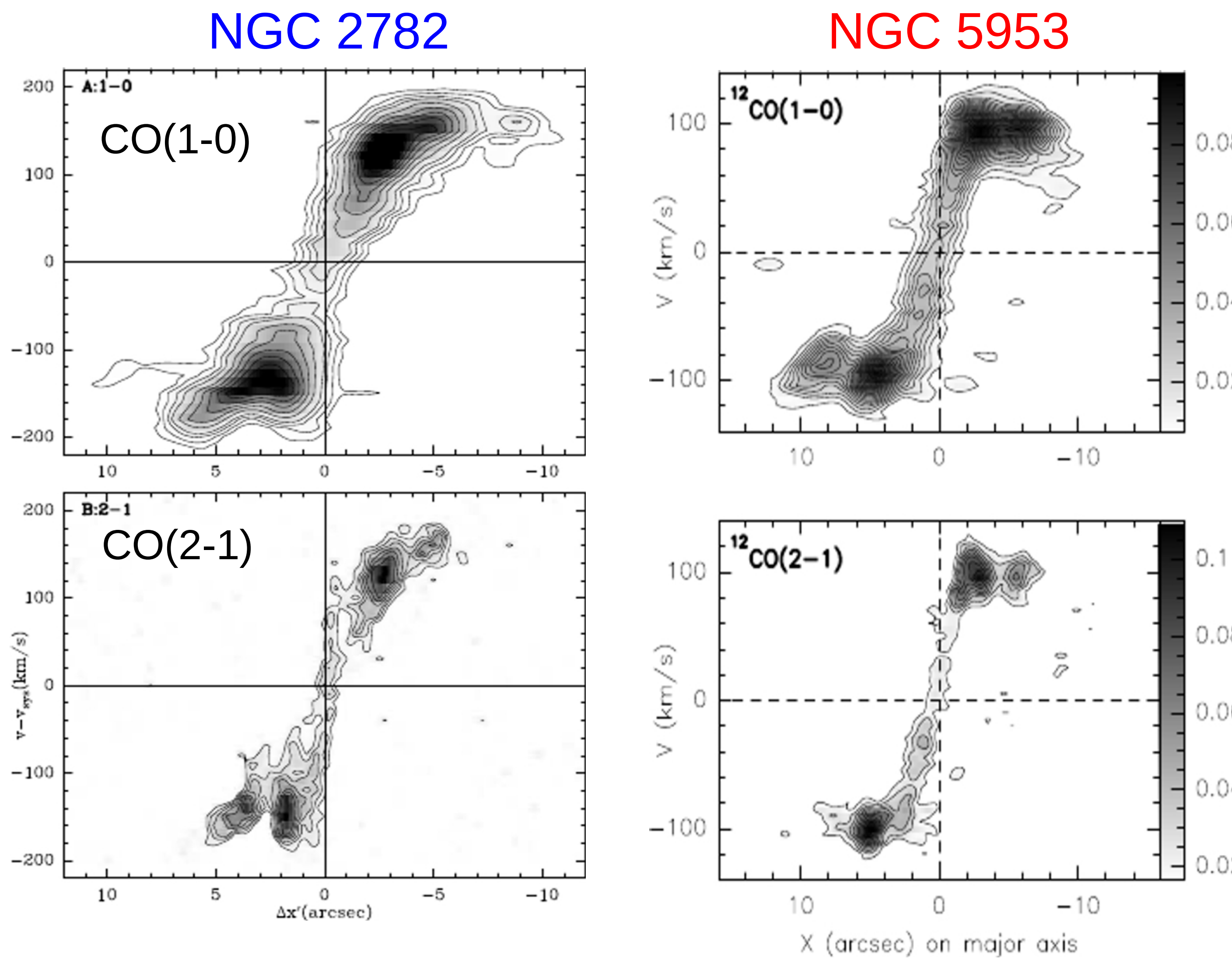

Signature of rotating disk clear in both galaxies

Observed major-axis PV diagrams

NGC 2782 — NGC 5953

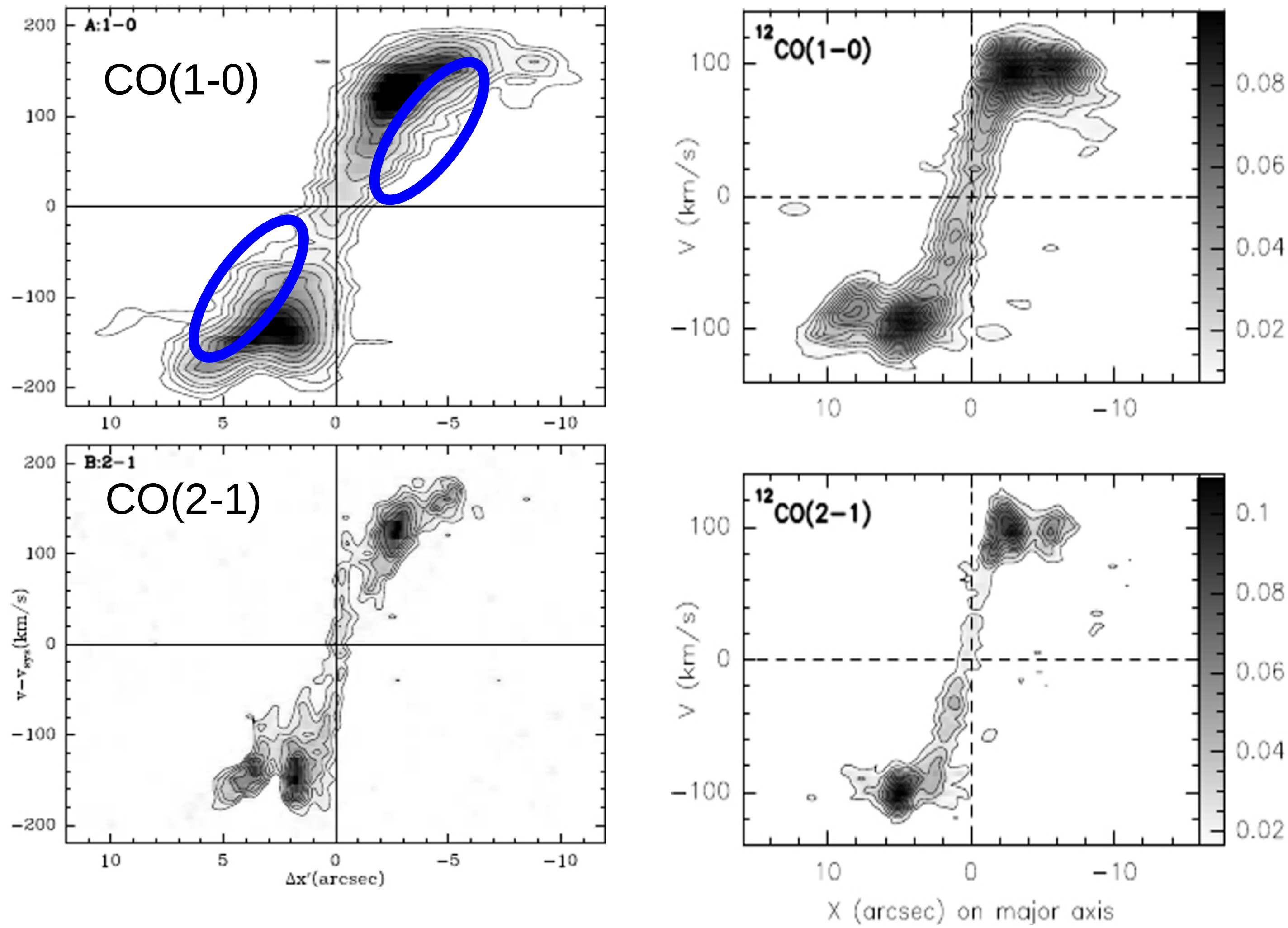

Signature of rotating disk clear in both galaxies, but non-circular streaming motions evident in NGC 2782

Rotation curves

Rotation (or “circular-velocity”) curves are defined as the trace of velocities on a major-axis PV diagram, correcting for the angle between the line of sight and the galaxy disk (inclination).

NGC 5953

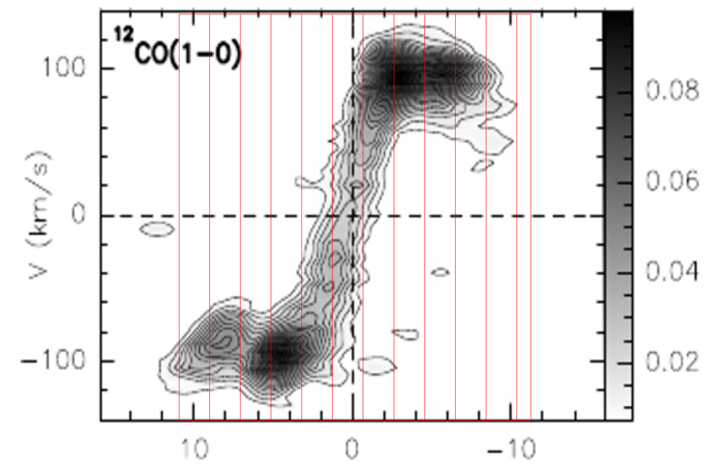

Distance in arcsec along the major axis

Intensity-weighted velocities:

$$V_{int} = \int I(v)\, v\, dv \;\Big/ \int I(v)\, dv$$

Rotation curves

Rotation (or “circular-velocity”) curves are the trace of velocities on a major-axis PV diagram, correcting for the angle between the line of sight and the galaxy disk (inclination).

Intensity-weighted velocities:

$$V_{int} = \int I(v)\, v\, dv \;\Big/ \int I(v)\, dv$$

approximated by ***Gaussian fits for each radial bin*** *(and take the velocity with the most intense component in messy situations with multiple velocity peaks)*

NGC 5953

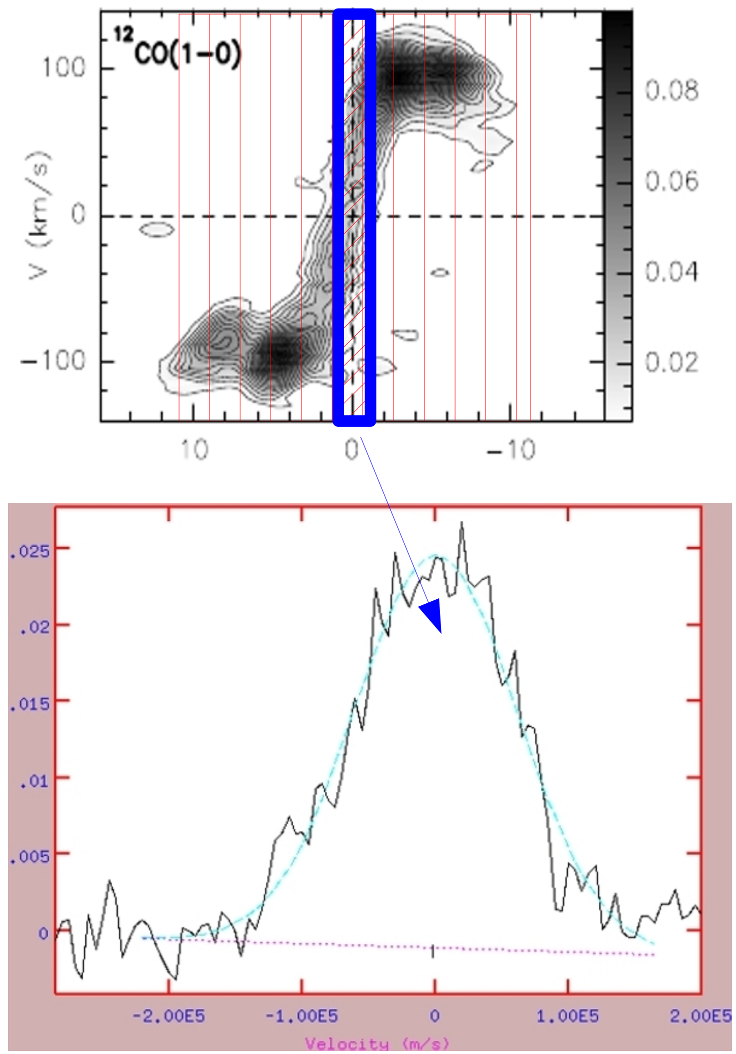

Velocity (km/s)

Rotation curves

NGC 5953pc (28 Mpc, 1”=136pc)

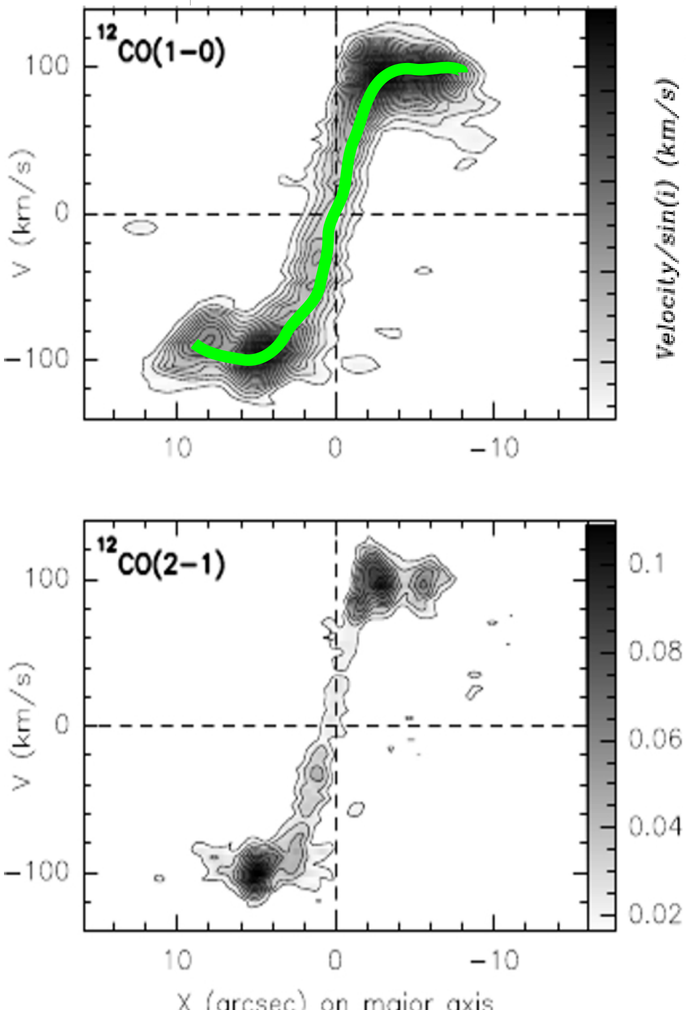

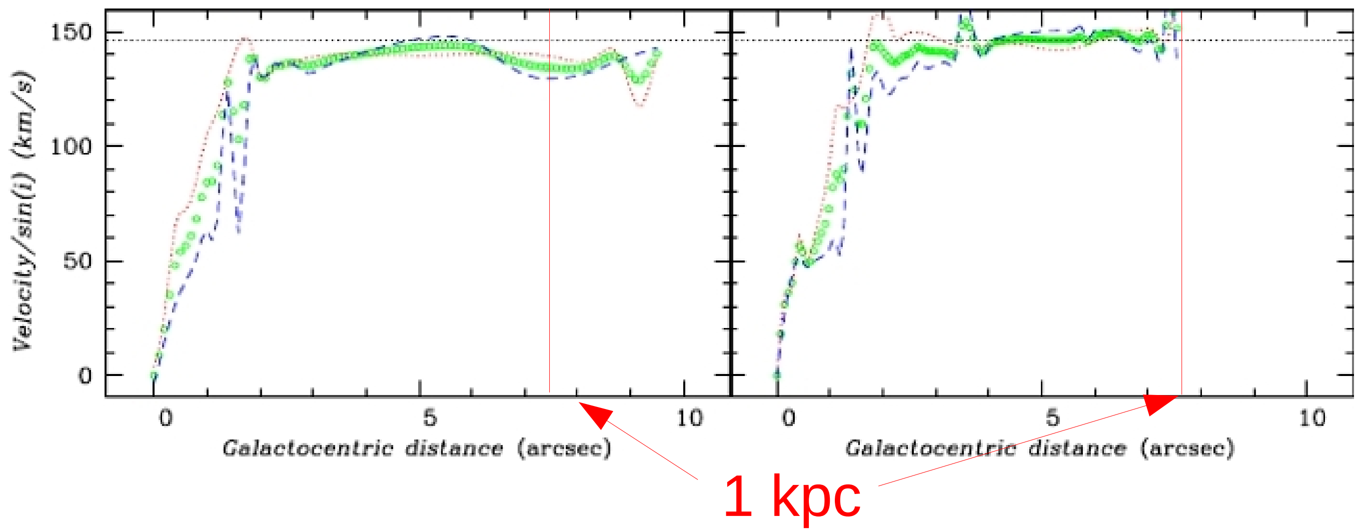

Average of postive and negative velocities about the rotation axis

CO rotation curves useful only for circumnuclear region where the molecular is the dominant component; but high resolution has diagnostic power.

HI traces the outer disk more effectively (extending the flat part of the rotation curve).

Rotation curves

NGC 2782 (35 Mpc, 1” = 171 pc)

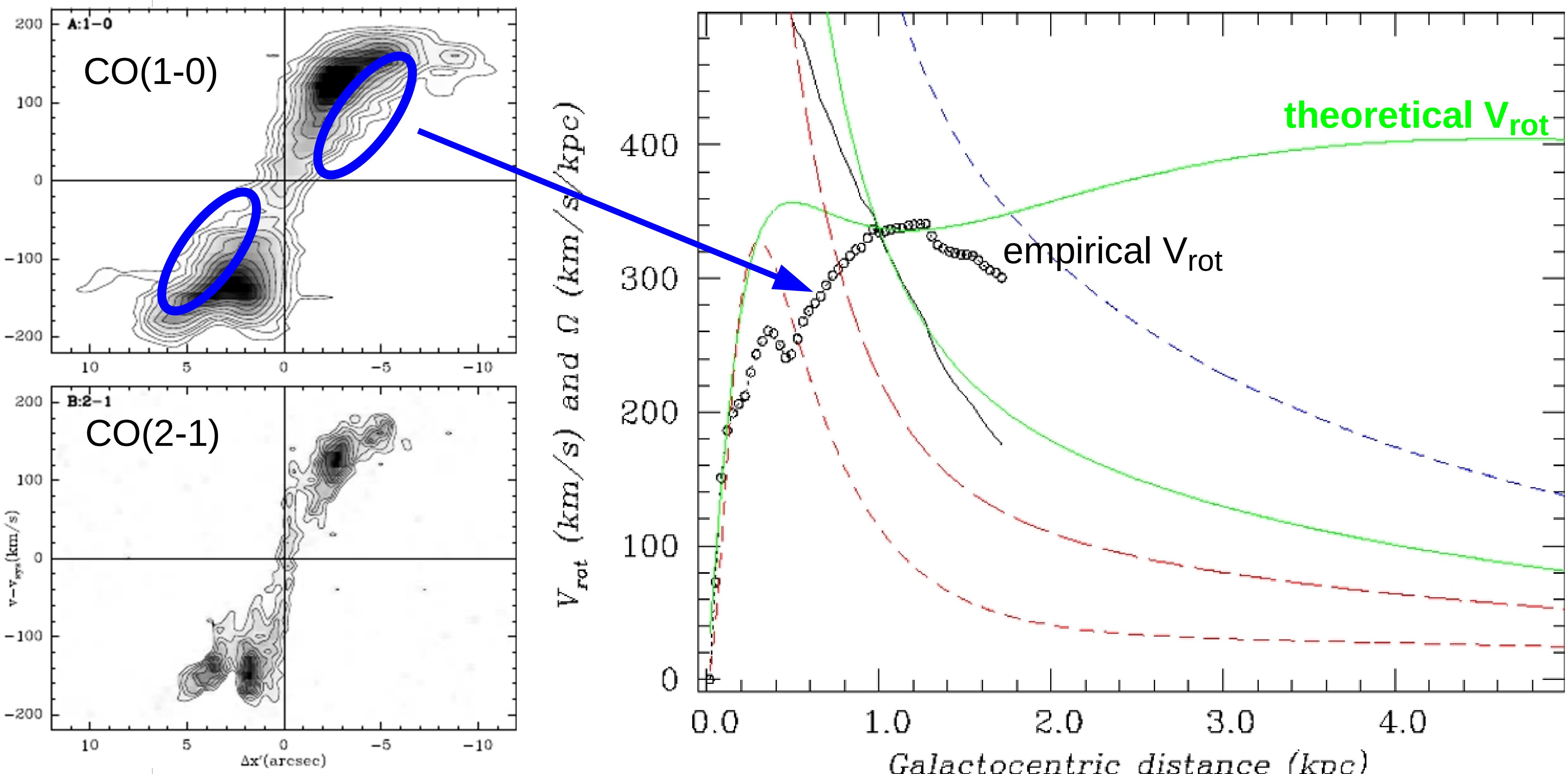

Circumnuclear gas may not always trace circular motions; *in NGC 2782, streaming motions between 200 and 800 pc...*

Rotation curves and resonances

Identify *non-axisymmetric features in stellar image* (near-infrared) or gas map, and measure their length...

Where these i*ntersect with the rotation curve* may be *resonances!*

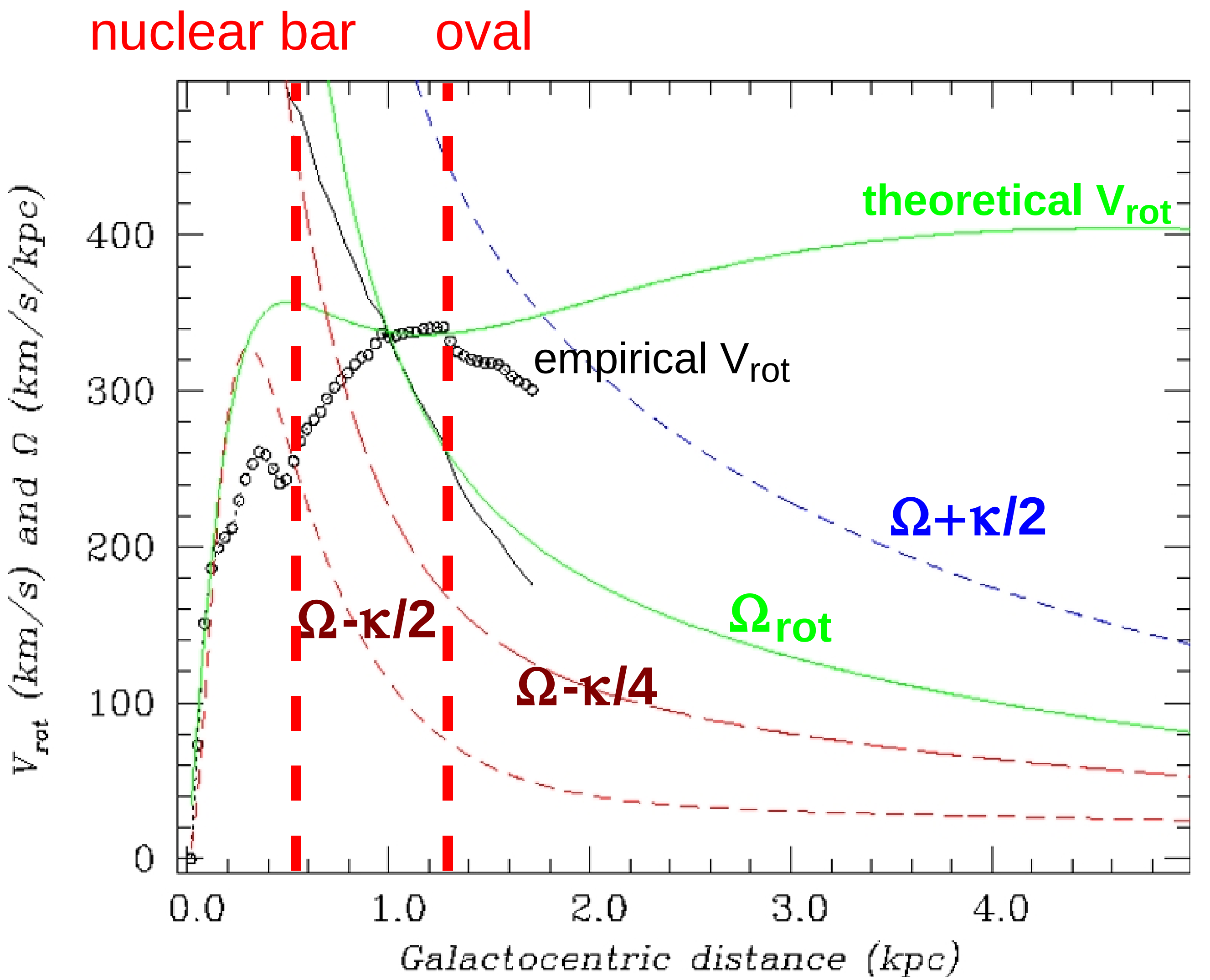

Rotation curves and resonances

Weak bar with pattern speed Ω_b in *epicyclic approximation,* epicyclic radial oscillation frequency:(see Binney & Tremaine 1987):

$$\boldsymbol{\Omega_{rot}^{\ 2}(R)} = 1/R\ (\ \partial\Phi/\partial R\ )$$

$$\boldsymbol{\kappa^2(R)} = R\ [d\Omega^2/dR + 4\Omega^2]$$

Lindblad resonances when

$$\mathbf{m(\Omega_{rot} - \Omega_{b}) = +/-\kappa}$$

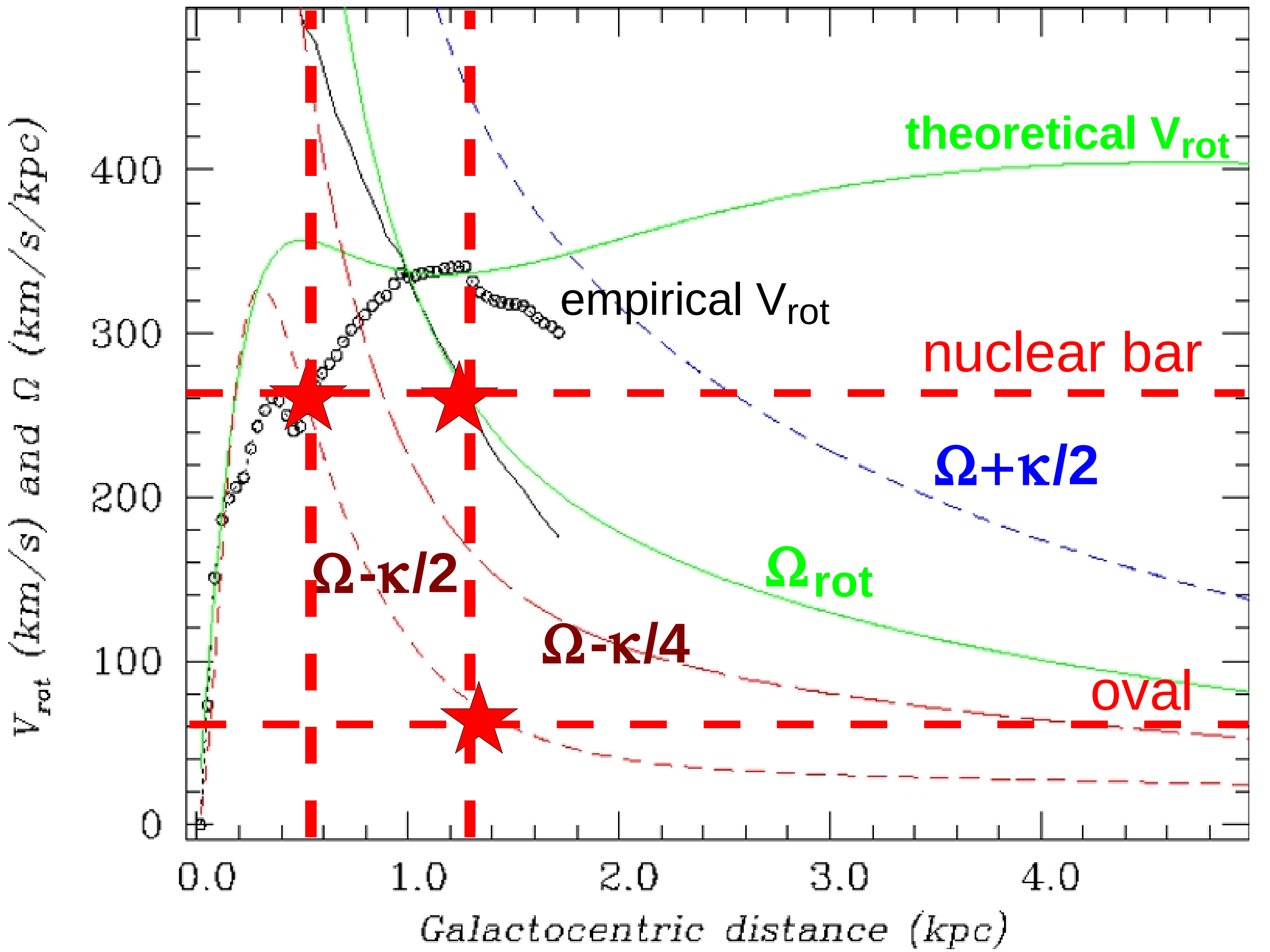

Inner Lindblad (ILR) and corotation resonances for nuclear bar (fast $\mathbf{\Omega_b}$) and oval (slow $\mathbf{\Omega_b}$)

Dynamical torques and AGN fueling

Power source of AGN is accretion onto a supermassive black hole (SMBH).

High luminosities and small spatial scales (<1pc) imply non-stellar power supply, thought to be accretion onto a deep gravitational potential.

Questions:

- What turns on the AGN? (only ~5% galaxies host AGN) ... and what turns it off again?
- How does the fuel, gas on kpc scales in the galaxy disk, lose its angular momentum and flow in to the event horizon scales around the SMBH?

CO and bars

Molecules important for tracing the dynamical action of bars (HI usually depleted in central regions)

Variety of morphologies:
rings, bars,
spiral structure

twin peaks leading
offset dust lanes

(Sakamoto+ 1999)

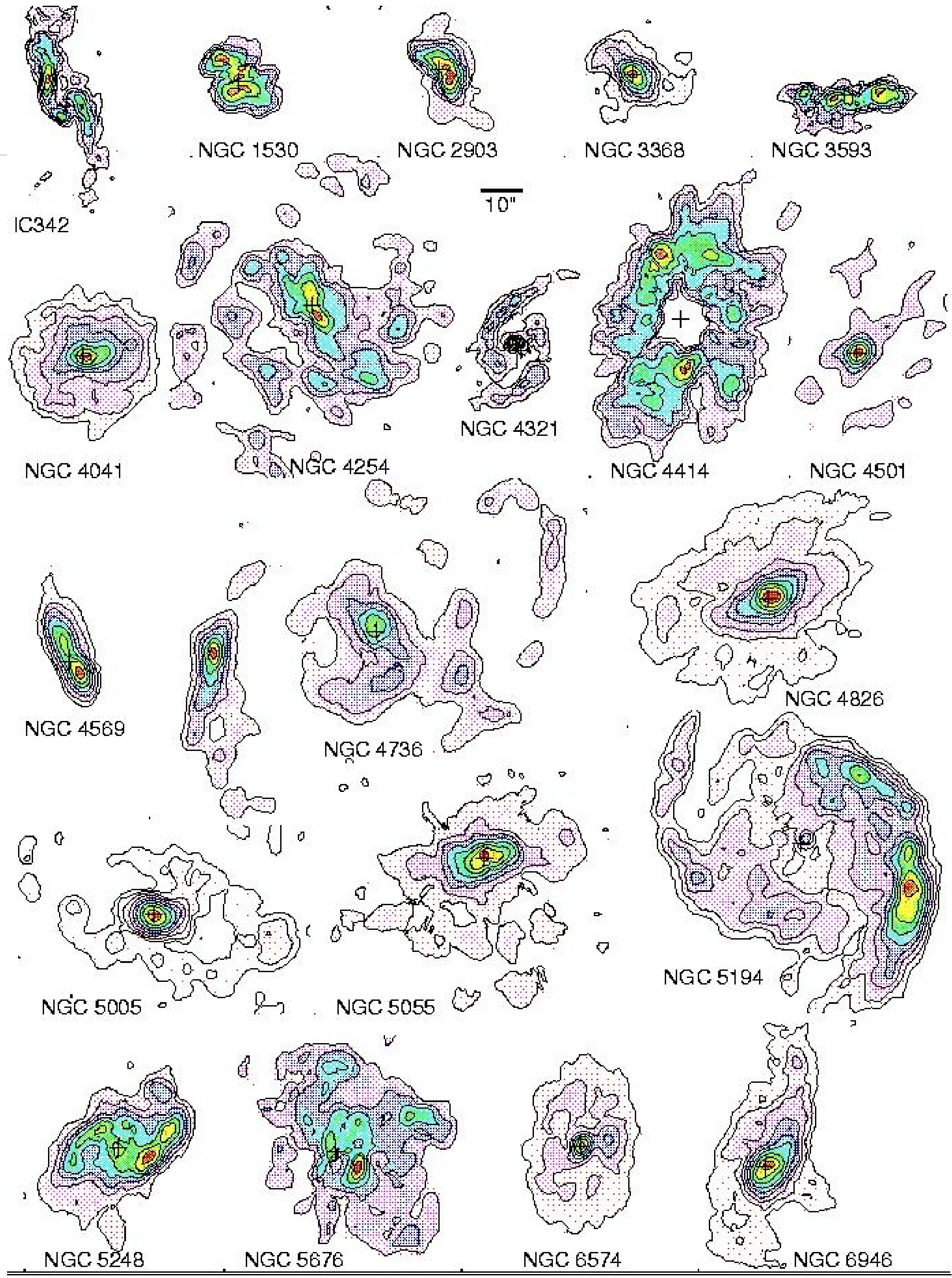

Where is the CO in barred galaxies?

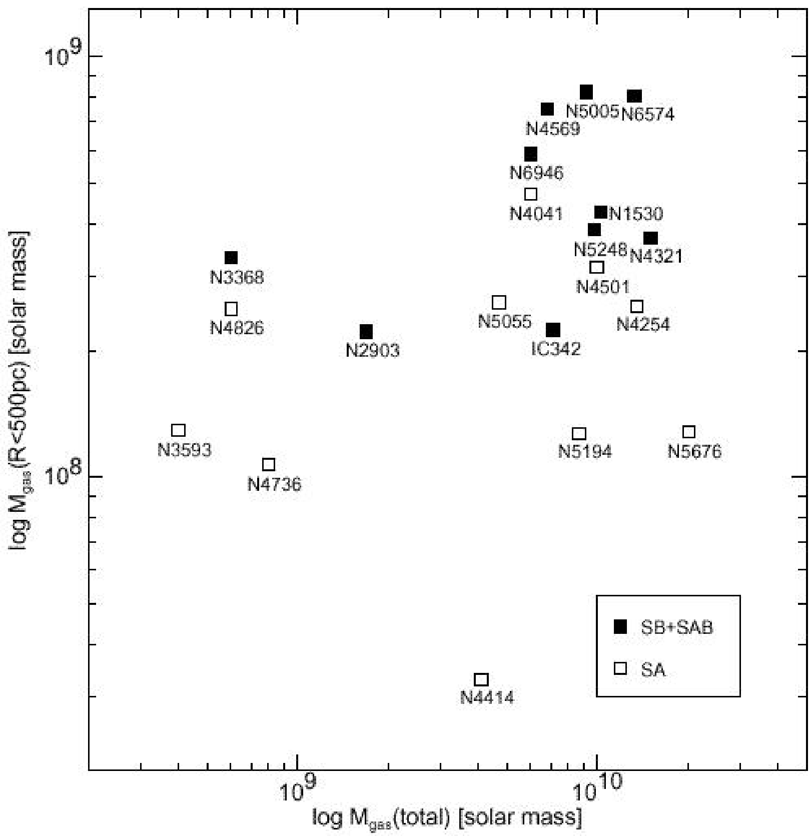

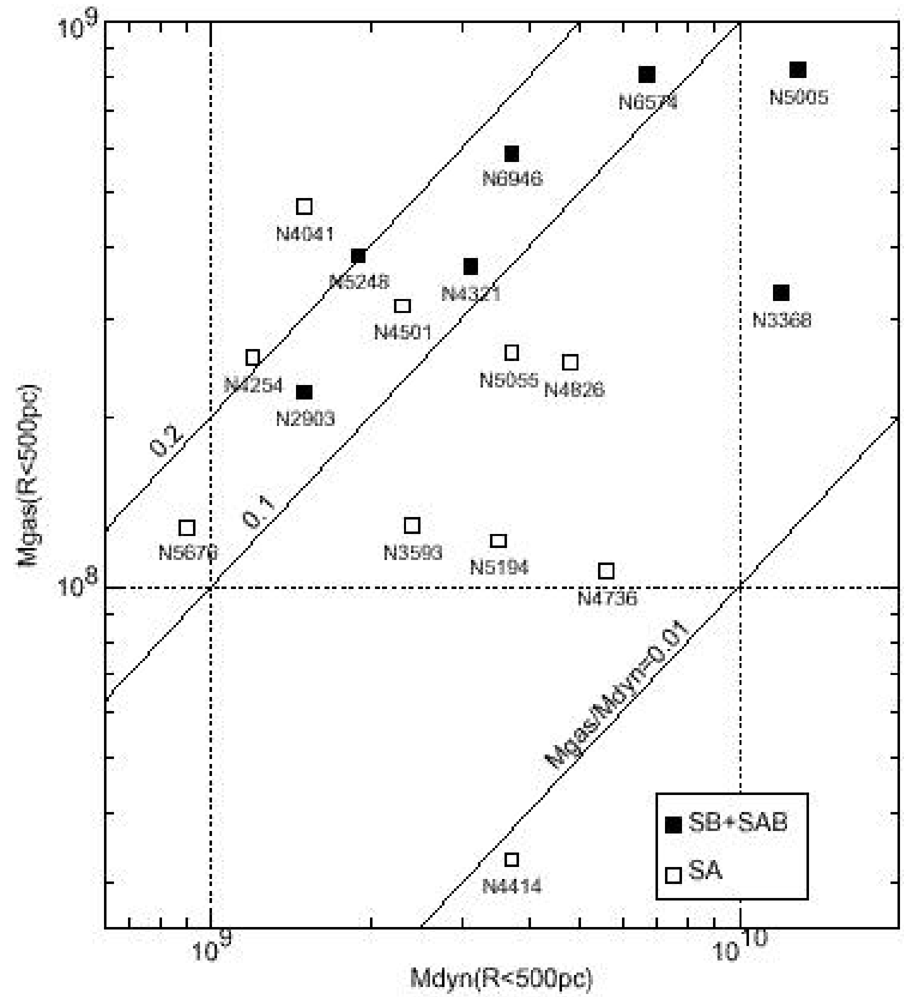

Relative to unbarred galaxies, CO emission in barred galaxies is more concentrated, and there is more gas (relative to dynamical mass) in central kpc scales...

But bars cannot overcome resonance barriers

- Theoretical and observational support for bar-driven gas transport, but no trend of more bars in low-luminosity (Seyfert) AGN!

- NUGA search for a ‘universal’ feeding agent in low-luminosity AGN unsuccessful. *Gas rings, nuclear gas bars, nuclear spiral arms, disks, and lopsidedness apparently unable to produce significant fueling on scales « 1 kpc.*

- *Usually gas gets stopped in at the* ***ILR barriers at ~a few 100 pc!***

- *So how can the gas* ***lose its angular momentum*** *to fuel the SMBH on small spatial scales?*

Examine torques on gas by gravitational potential from stars

Stellar potentials and gravity torque maps

Underlying assumptions (Garcia-Burillo+ 2005):

(1) Stellar mass distribution accurately estimated by near-infrared images
(2) Stars define the total gravitational potential acting on the gas

I. Derive potential

$$\boxed{\Phi(R,\theta) = \Phi_0(R) + \sum_m \Phi_m(R)\cos(m\theta - \phi_m)}$$

Stellar potentials and gravity torque maps

Underlying assumptions (Garcia-Burillo+ 2005):

(1) Stellar mass distribution accurately estimated by near-infrared images
(2) Stars define the total gravitational potential acting on the gas

I. Derive potential

$$\boxed{\Phi(R,\theta) = \Phi_0(R) + \sum_m \Phi_m(R)\cos(m\theta - \phi_m)}$$

II. Derive torque maps t(x,y)

$$\boxed{t(x,y) = (x.F_y - y.F_x)}$$

Stellar potentials and gravity torque maps

Underlying assumptions (Garcia-Burillo+ 2005):

(1) Stellar mass distribution accurately estimated by near-infrared images
(2) Stars define the total gravitational potential acting on the gas

I. Derive potential

$$\boxed{\Phi(R,\theta) = \Phi_0(R) + \sum_m \Phi_m(R)\cos(m\theta - \phi_m)}$$

II. Derive torque maps t(x,y)

$$\boxed{t(x,y) = (x.F_y - y.F_x)}$$

III. Average torque t(r) azimuthally and weight by column density

$$\boxed{t(r) = \frac{\int_\theta N(x,y)(x.F_y - y.F_x)}{\int_\theta N(x,y)}}$$

Stellar potentials and gravity torque maps

Underlying assumptions (Garcia-Burillo+ 2005):

(1) Stellar mass distribution accurately estimated by near-infrared images
(2) Stars define the total gravitational potential acting on the gas

I. Derive potential

$$\Phi(R,\theta) = \Phi_0(R) + \sum_m \Phi_m(R)\cos(m\theta - \phi_m)$$

II. Derive torque maps t(x,y)

$$t(x,y) = (x.F_y - y.F_x)$$

III. Average torque t(r) azimuthally and weight by column density

$$t(r) = \frac{\int_\theta N(x,y)(x.F_y - y.F_x)}{\int_\theta N(x,y)}$$

IV. Derive efficiencies

$$\epsilon = dL/dt \times 1/L \times T_{rot} = t(r)/L \times T_{rot}$$

AGN fueling elusive

Most NUGA galaxies have *positive torques t(r) > 0 at r < 200pc*
→ stellar torques inefficient at driving gas inflow in the present epoch!   How can AGN be fueled if currently no gas is being driven inward?

Short-lived (<10^7 yrs) feeding agent in stellar potential?
"*Smoking-gun" (gas inflow on small spatial scales) elusive!*

But negative torques found in torque maps of NGC 2782:

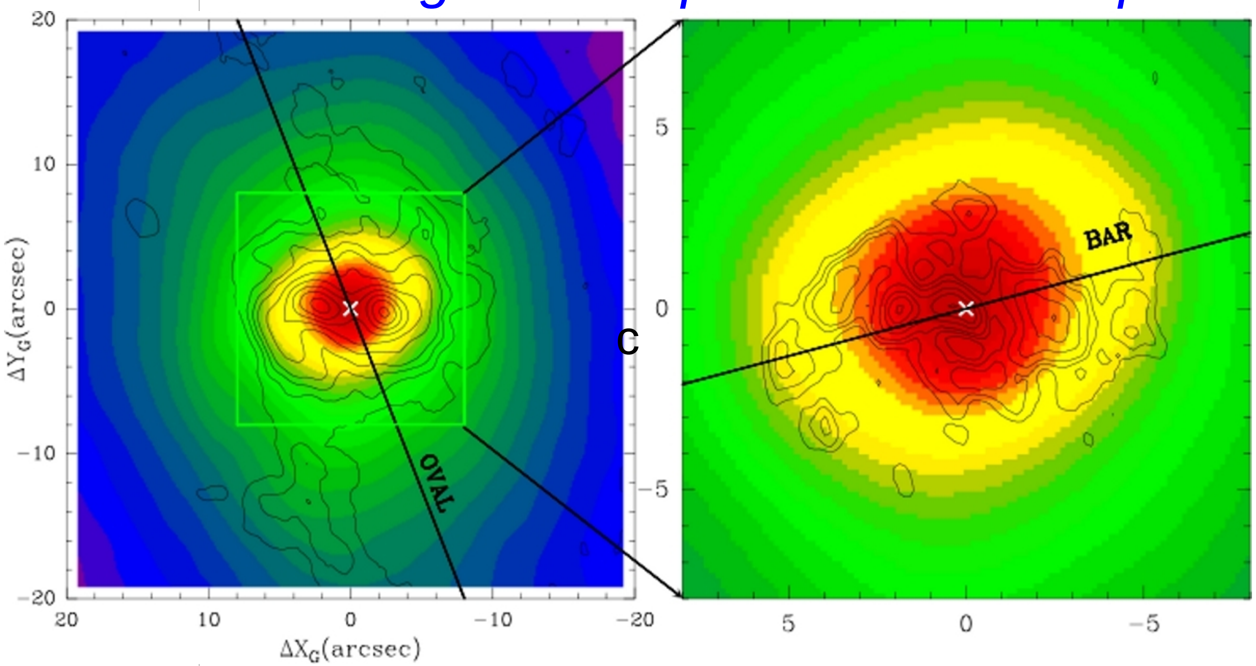

Stellar potential (see left) shows two embedded bars (remember RC)

Nuclear bar decoupling
→ molecular gas inside ILR(oval)

“Smoking-gun evidence” in NGC 2782

Numerical simulations for NGC 2782

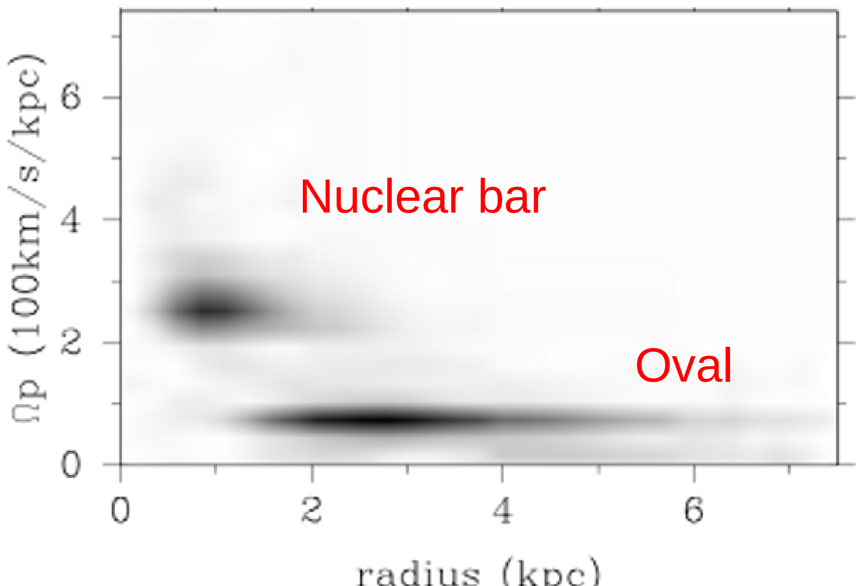

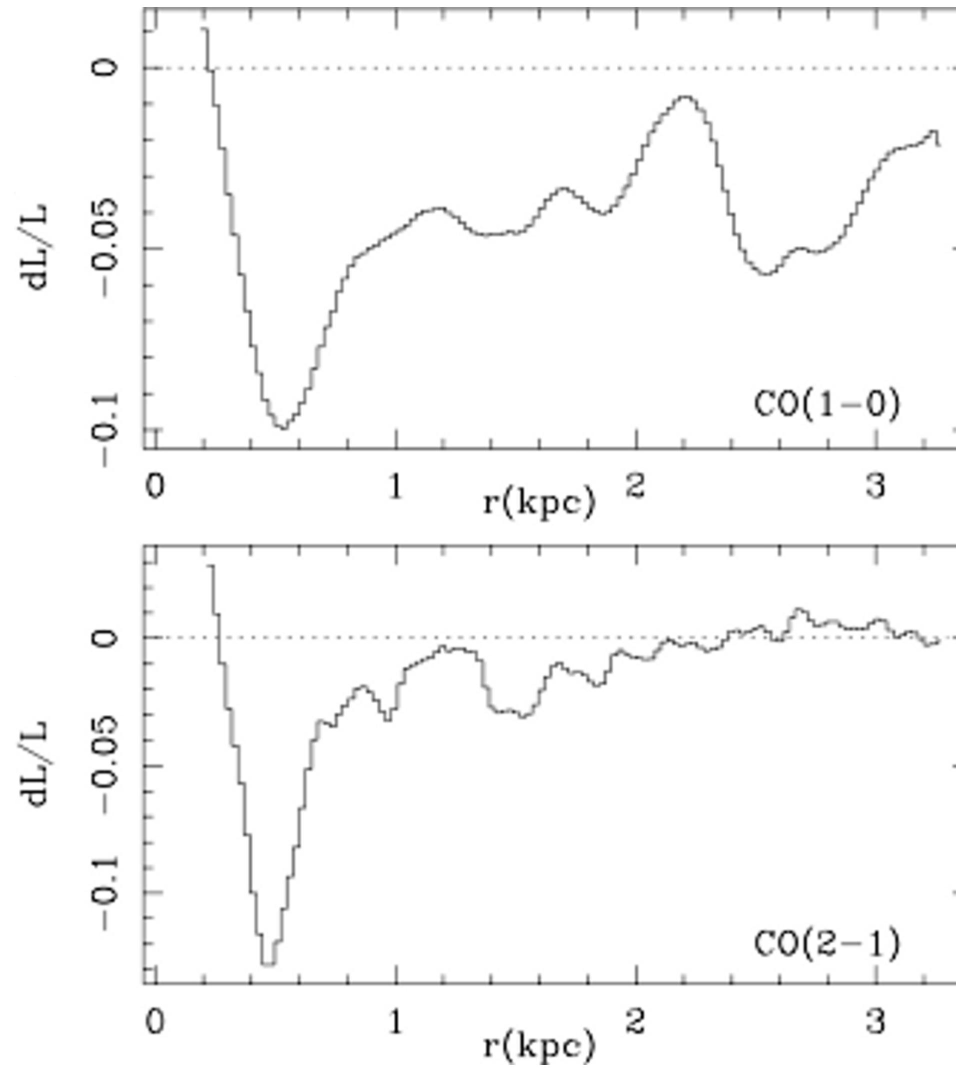

Stellar potential shows two embedded bars with different pattern speeds Ω_p (remember RC)

Dynamical decoupling → molecular gas inside ILR(oval)

Hunt+ (2008)

“Smoking-gun evidence” in NGC 2782

Numerical simulations for NGC 2782

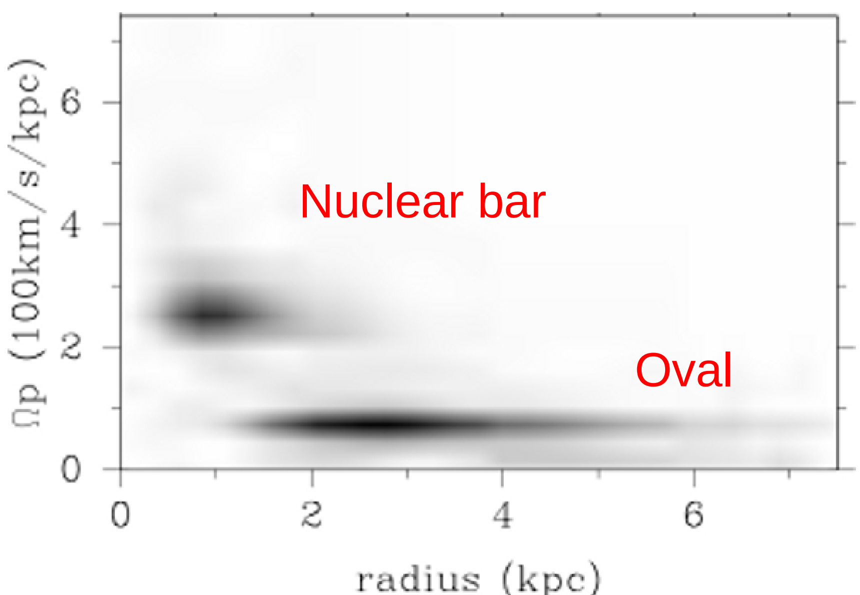

Stellar potential shows two embedded bars with different pattern speeds Ω_p (remember RC)

Dynamical decoupling → molecular gas inside ILR(oval) → “smoking gun”!

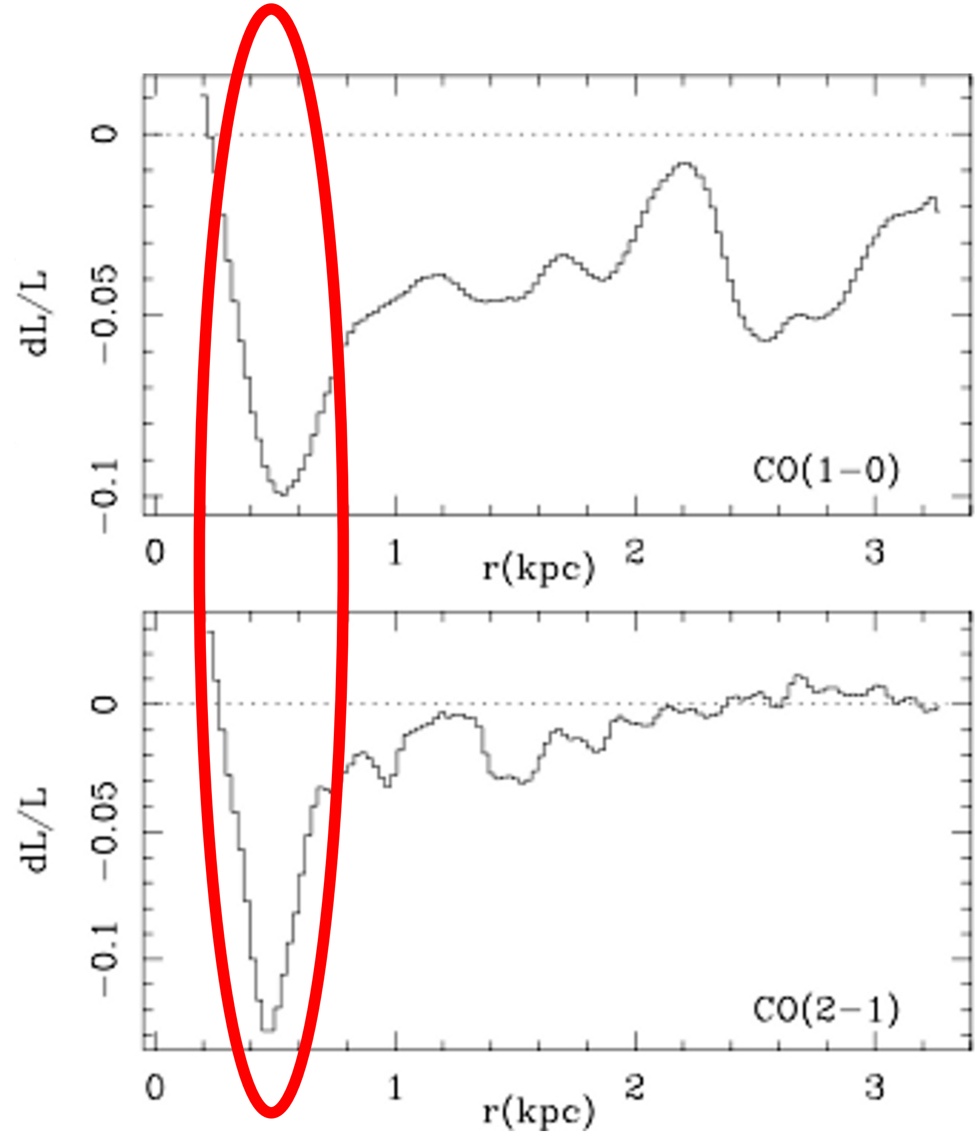

Hunt+ (2008)

Molecular gas kinematics in nuclei of galaxies

- Although HI and ionized gas also effective kinematic tracers, CO uniquely useful to trace circumnuclear regions of galaxies because such regions are **dusty** (extinction a problem for ionized gas tracers)**,** and usually devoid of HI (and CO maps have better spatial resolution than HI.)
- Barred galaxies show higher concentration of molecular gas than unbarred galaxies (Sakamoto+ 1999), confirming dynamical theories which suggest that bars transport gas inward.
- Analysis of gravitational potential, resonances, and torques (Garcia-Burillo+ 2005) enable estimate of net gas inflow and outflow to circumnuclear regions, to fuel AGN and star formation. 6/12 analyzed NUGA galaxies show inflow!
- Streaming motions are ambiguous signatures of inflow... Gravity could be assisted by other mechanisms such as viscosity and dynamical friction...

III (a). (Some) Other molecules

High-density molecular tracers

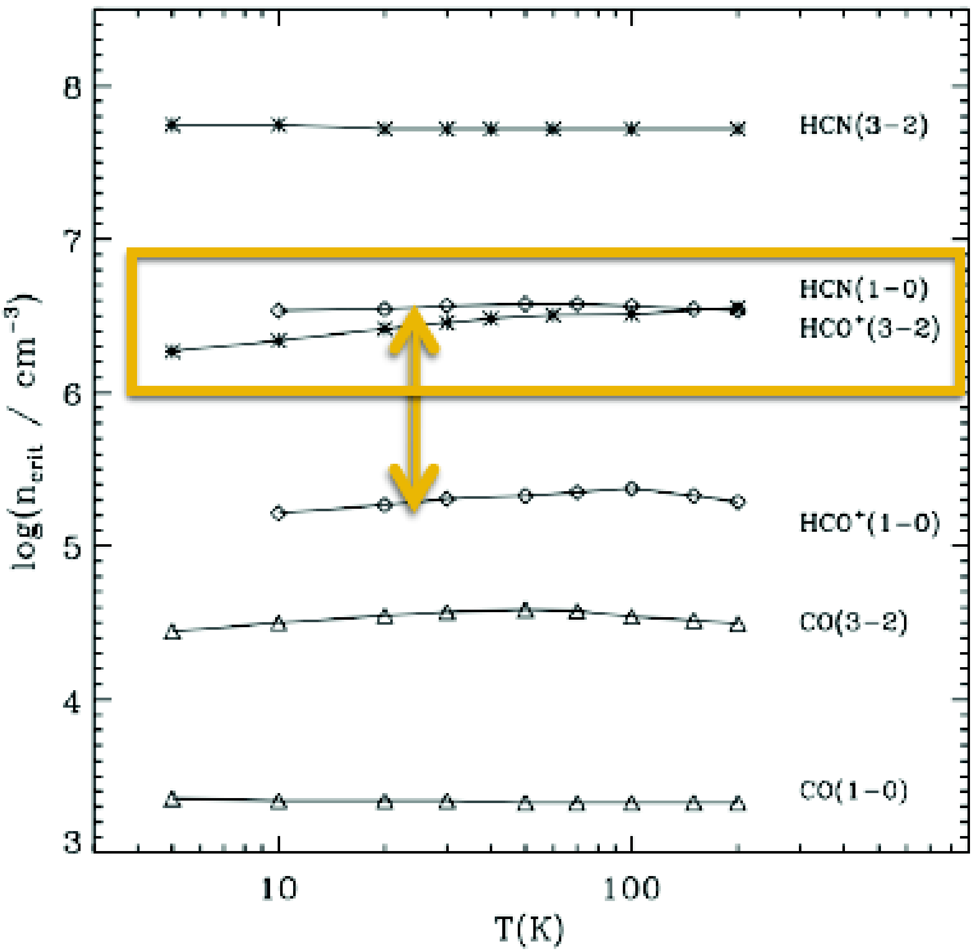

Competition between radiative and collisional de-excitation quantified by ratio C_{ul}/A_{ul}

$A_{J-1\neg J} \sim J^3 \mu_{el}^2$, where μ_{el} = electric dipole moment, J = angular momentum quantum number

Critical density n_{crit} for which C_{ul}/A_{ul} = 1 ~ $n(H_2)T^{1/2} / J^3 \mu_{el}^2$

*Because of their higher n_{crit} molecules with larger μ_{el} (and higher-order transitions) trace **hotter/denser** molecular gas.*

High-density molecular tracers: HCN(1-0)

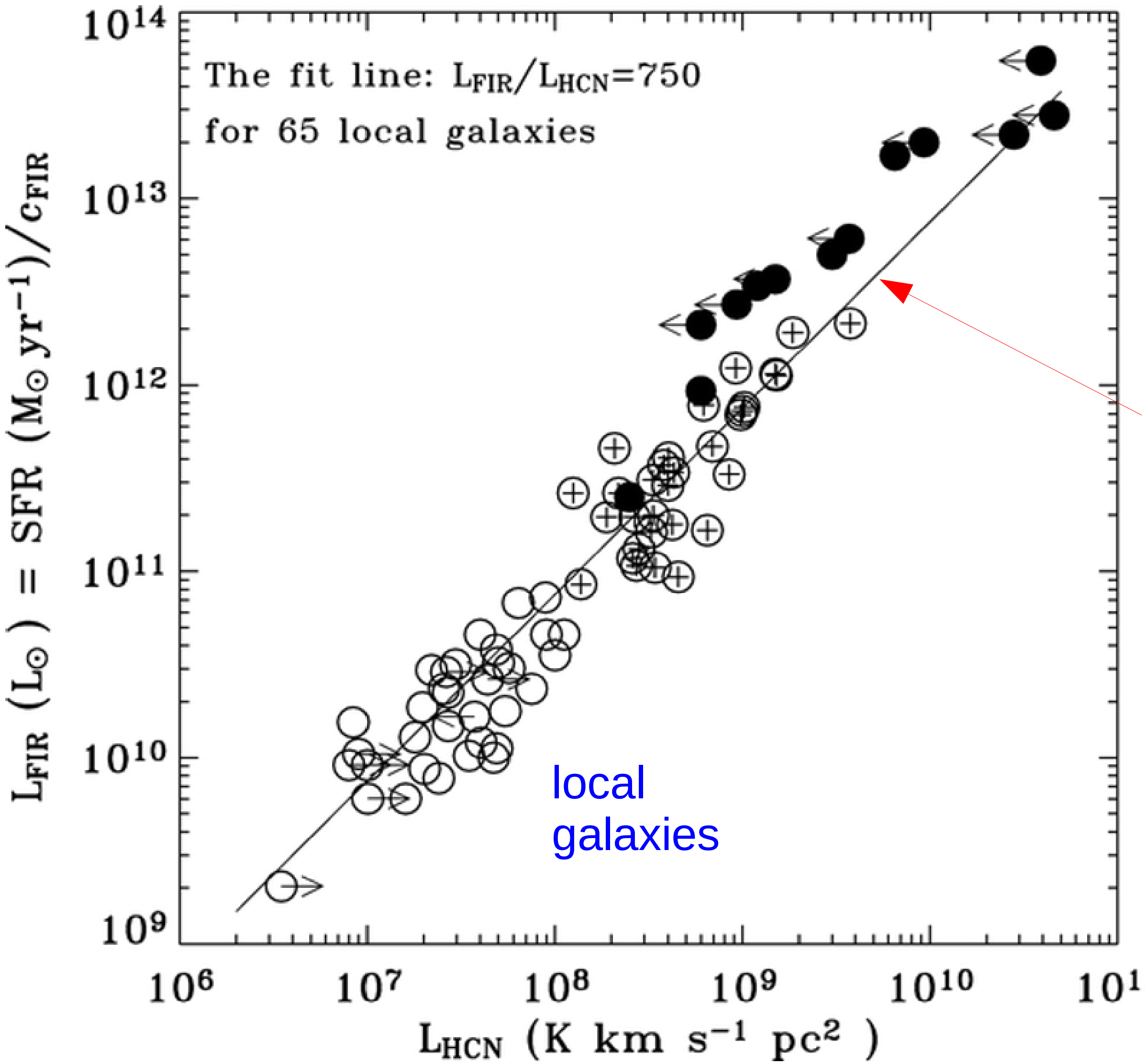

high-redshift sub-millimeter galaxies

slope = 1

Linear (rather than super-linear as for CO); dense gas more closely correlated with star formation.

Correlation between IR (~ SFR) and HCN J=1-0 luminosity (~mass of gas above critical density) (Gao & Solomon 2004, Gao+ 2007, see also Wu+ 2005)

High-density tracers: HCO^+

HCN(1-0)/HCO+(1-0)

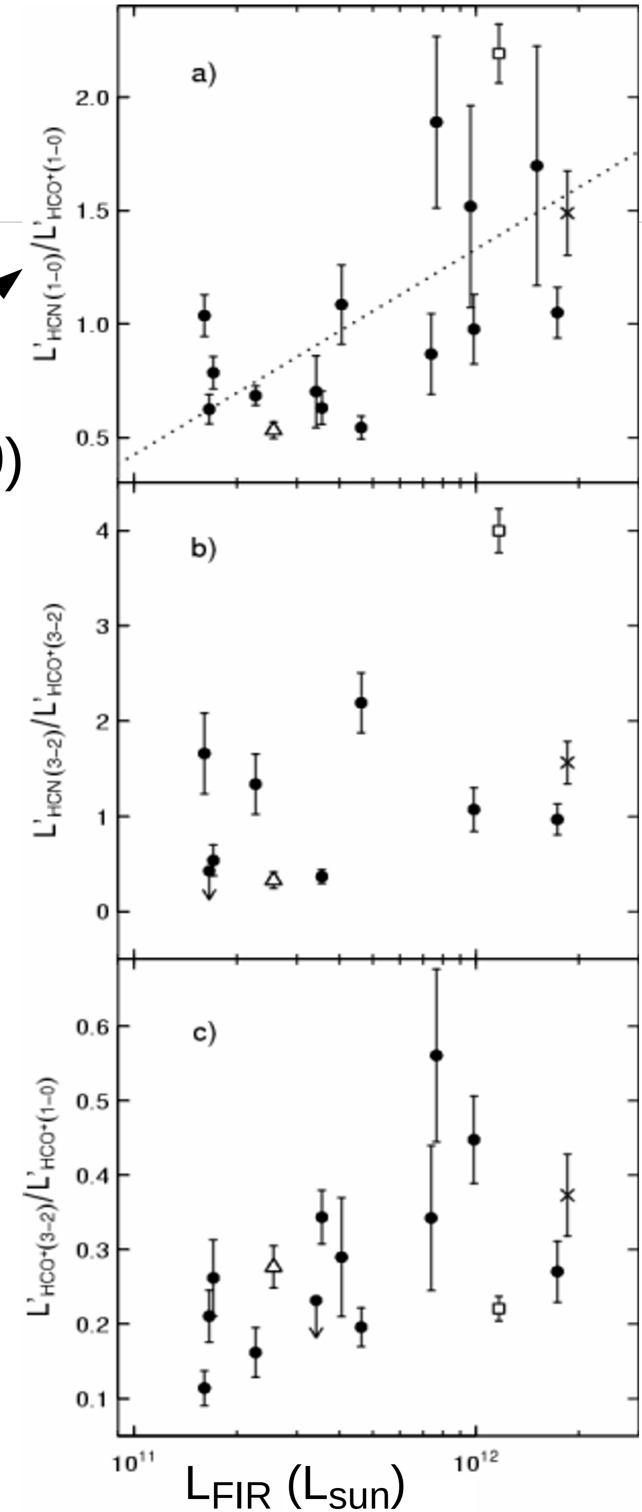

But at high densities (and high $L_{IR} \geq 10^{11}$ L_{sun}), because of its higher n_{crit} HCN(1-0) may be enhanced over other dense-gas tracers such as HCO^+ (Garcia-Carpio+ 2006, 2008).

Optically thin molecular tracers: ^{13}CO

^{12}C/^{13}C $\cong$ 50-70, i.e. rare; ^{13}C likely optically thin. Thus, unlike ^{12}CO which is optically thick, ^{13}CO can be used to infer column densities N(^{13}CO) and N(^{12}CO), because of the relation between N and τ.

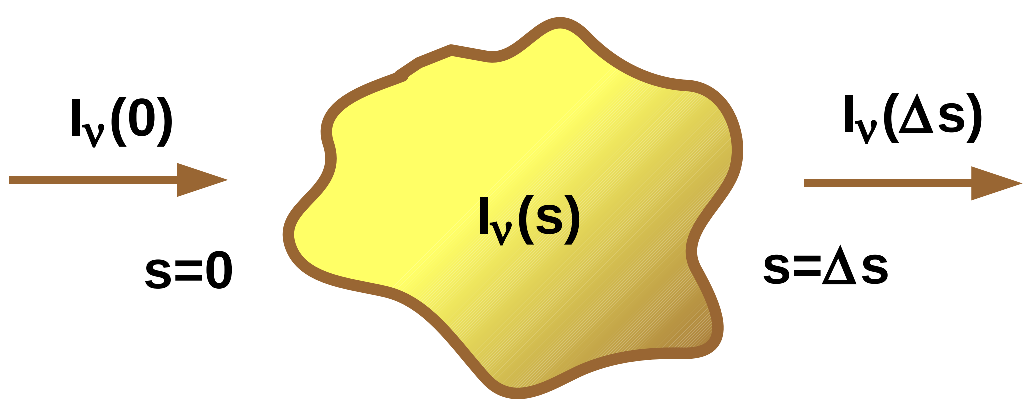

observer

Optical depth:
$\Delta\tau_\nu = \alpha_\nu \, \Delta s$

I_ν = *spectral intensity*, j_ν = *spectral emission coefficient*, $\boldsymbol{\alpha_\nu}$ = *spectral absorption coefficient.*

***Radiation transfer equation*:**

$$\frac{dI_\nu}{ds} = -\alpha_\nu \, I_\nu + j_\nu$$

Radiation transfer and thermal emission

After dividing by α_ν, and substituting for τ_ν, the transfer equation can be written as:

$$\frac{dI_\nu}{d\tau_\nu} = -I_\nu + S_\nu$$

where the "source function" S_ν defined as: $$S_\nu \equiv \frac{j_\nu}{\alpha_\nu}$$

Thus, solution is:

$$I_\nu(\Delta s) = I_\nu(0)e^{-\tau_\nu} + \frac{j_\nu}{\alpha_\nu}\left[1 - e^{-\tau_\nu}\right]$$

For *thermal emission:* $j_\nu = \alpha_\nu B_\nu(T)$ (Kirchoff's Law)

and solution becomes:

$$I_\nu(\Delta s) = I_\nu(0)e^{-\tau_\nu} + \frac{2h\nu^3/c^2}{\exp(h\nu/k_B T) - 1}\left[1 - e^{-\tau_\nu}\right]$$

Radiation transfer and thermal emission

After dividing by α_ν, and substituting for τ_ν, the transfer equation can be written as:

$$\frac{dI_\nu}{d\tau_\nu} = -I_\nu + S_\nu$$

where the "source function" S_ν defined as: $S_\nu \equiv \frac{j_\nu}{\alpha_\nu}$

Thus, solution is:

$$I_\nu(\Delta s) = I_\nu(0)e^{-\tau_\nu} + \frac{j_\nu}{\alpha_\nu}\left[1 - e^{-\tau_\nu}\right]$$

For *thermal emission:* $j_\nu = \alpha_\nu B_\nu(T)$ (Kirchoff's Law)

and solution becomes:

$$I_\nu(\Delta s) = I_\nu(0)e^{-\tau_\nu} + \frac{2h\nu^3/c^2}{\exp(h\nu/k_BT) - 1}\left[1 - e^{-\tau_\nu}\right]$$

Radiative transfer and brightness temperature T_B

Rayleigh-Jeans approximation for low-energy transitions hν « kT_B so that transfer equation becomes:

$$T_B(\Delta s) = T_B(0)e^{-\tau_\nu(\Delta s)} + T[1 - e^{-\tau_\nu(\Delta s)}]$$

Relate ***differences in intensity*** to ***the measurement unit of*** *brightness temperature,* ***T_B,*** and *observed antenna temperature,* ***T_A,*** via the Planck function:

$$T_B \equiv \frac{c^2}{2\nu^2 k_B}[I_\nu(\Delta\tau_\nu) - I_\nu(0)]$$

$$T_B = \frac{T_A}{\eta}\left(\frac{\theta^2_{source} + \theta^2_A}{\theta^2_{source}}\right)$$

where η = main beam efficiency;
θ_A, θ_{source} = beam, source size

Conversion from T_A to T_B depends on source size!

Radiative transfer and "detection equation"

Assuming baseline subtracted (so omit term behind cloud), and remembering that cosmic background radiation is everywhere, we have the difference of two intensities as the *"detection equation"* (see Stahler & Palla 2004; Wilson, Rohlfs, & Hüttemeister 2009):

$$T_B(\nu) = T_0 \left(\frac{1}{e^{T_0/T_{ex}} - 1} - \frac{1}{e^{T_0/2.7} - 1} \right) (1 - e^{-\tau_\nu})$$

where $T_0 = h\nu/k$ [5.5K for $^{12}CO(1\text{-}0)$, 5.3K $^{13}CO(1\text{-}0)$].

Radiative transfer and "detection equation"

Assuming baseline subtracted (so omit term behind cloud), and remembering that cosmic background radiation is everywhere, we have the difference of two intensities as the *"detection equation"* (see Stahler & Palla 2004; Wilson, Rohlfs, & Hüttemeister 2009):

$$T_B(\nu) = T_0 \left(\frac{1}{e^{T_0/T_{ex}} - 1} - \frac{1}{e^{T_0/2.7} - 1} \right) (1 - e^{-\tau_\nu})$$

where $T_0 = h\nu/k$ [5.5K for $^{12}CO(1\text{-}0)$, 5.3K $^{13}CO(1\text{-}0)$].

One observable for each line: $T_B(\nu)$

Radiative transfer and "detection equation"

Assuming baseline subtracted (so omit term behind cloud), and remembering that cosmic background radiation is everywhere, we have the difference of two intensities as the *"detection equation"* (see Stahler & Palla 2004; Wilson, Rohlfs, & Hüttemeister 2009):

$$T_B(\nu) = T_0 \left(\frac{1}{e^{T_0/T_{ex}} - 1} - \frac{1}{e^{T_0/2.7} - 1} \right) (1 - e^{-\tau_\nu})$$

where $T_0 = h\nu/k$ [5.5K for $^{12}CO(1\text{-}0)$, 5.3K $^{13}CO(1\text{-}0)$].

One observable for each line: $T_B(\nu)$

Two unknowns for each line: T_{ex} and τ_ν

τ_ν proportional to α_ν, hence to total volume density; Because of the Δs dependence, we can then infer column density!

Column density and optical depth of ^{13}CO

Hence need *two observables (^{13}CO and ^{12}CO)* and *some assumptions:*

- ✔ Uniform T_{ex} along the line of sight for J=1 → 0 transition, and CO lines emitted from the same volume
- ✔ Same T_{ex} for ^{13}CO and ^{12}CO
- ✔ $T_{kin}=T_{ex}$ for ^{12}CO, and $\tau(^{12}\mathrm{CO}) \gg 1$
- ✔ $\tau(^{13}\mathrm{CO}) \ll 1$

Recipe

(1) Derive T_{ex} for ^{12}CO(1-0) by assuming $\tau(^{12}\mathrm{CO}) \gg 1$ in detection equation

(2) With T_{ex}, detection equation can be solved for $\tau(^{13}\mathrm{CO})$

(3) $N(^{13}\mathrm{CO}) \sim \tau(^{13}\mathrm{CO})\ f(T_B, T_{ex}, A_{ul}, \text{partition})$

(4) $N(^{12}\mathrm{CO})/N(^{13}\mathrm{CO}) = \tau(^{12}\mathrm{CO})/\tau(^{13}\mathrm{CO})$

$N(^{12}\mathrm{CO}) = N(^{13}\mathrm{CO})\ \gamma\ [^{12}\mathrm{C}/^{13}\mathrm{C}]$, where $\gamma<1$ (fractionation, shielding)

III (b). Molecule content at low metallicity

CO deficit in low-metallicity dwarf galaxies

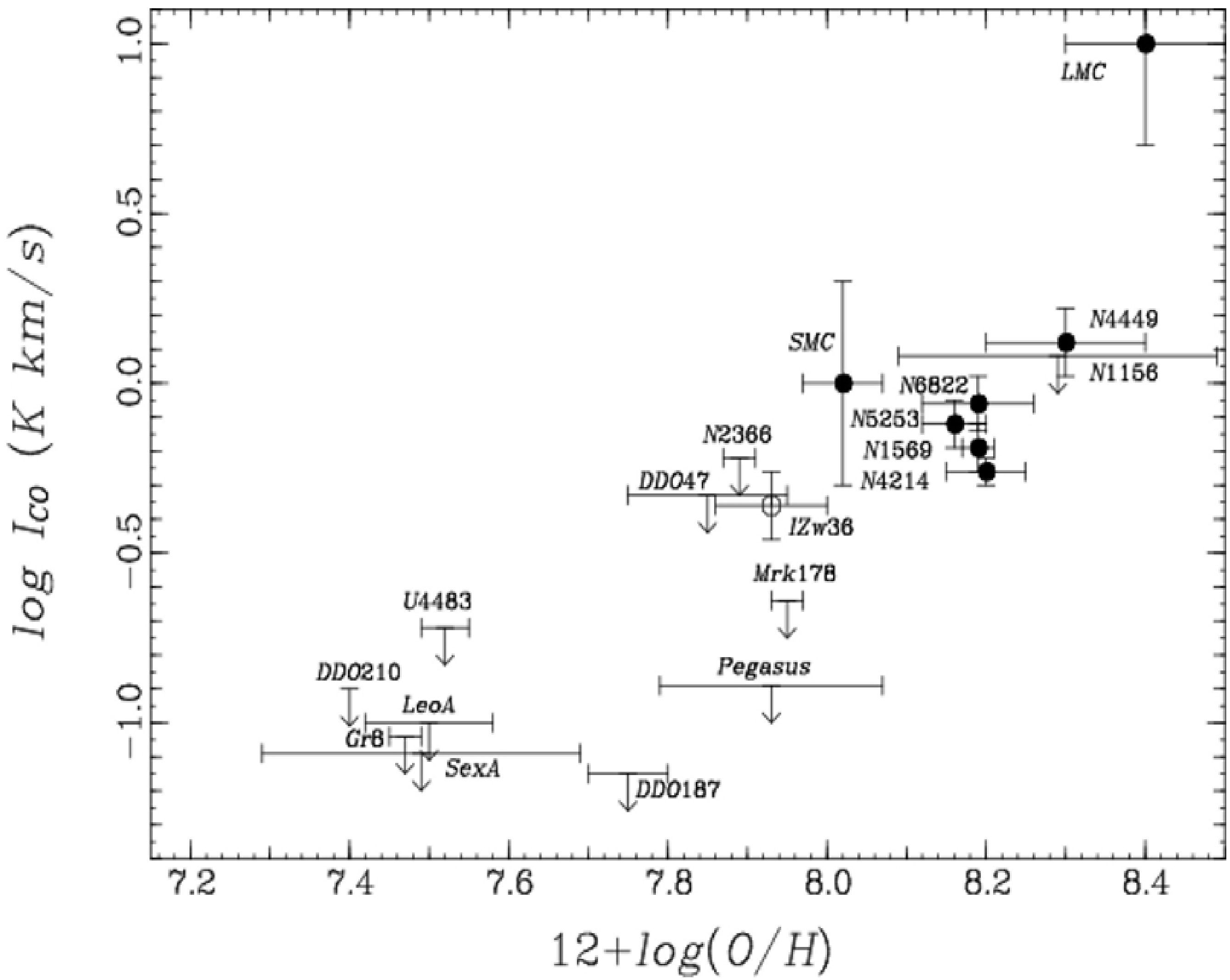

CO intensity vs. oxygen abundance (Taylor+ 1998). Below 12+logO/H ~ 8, virtually impossible to find CO!

Variation with O/H of CO conversion factor X?

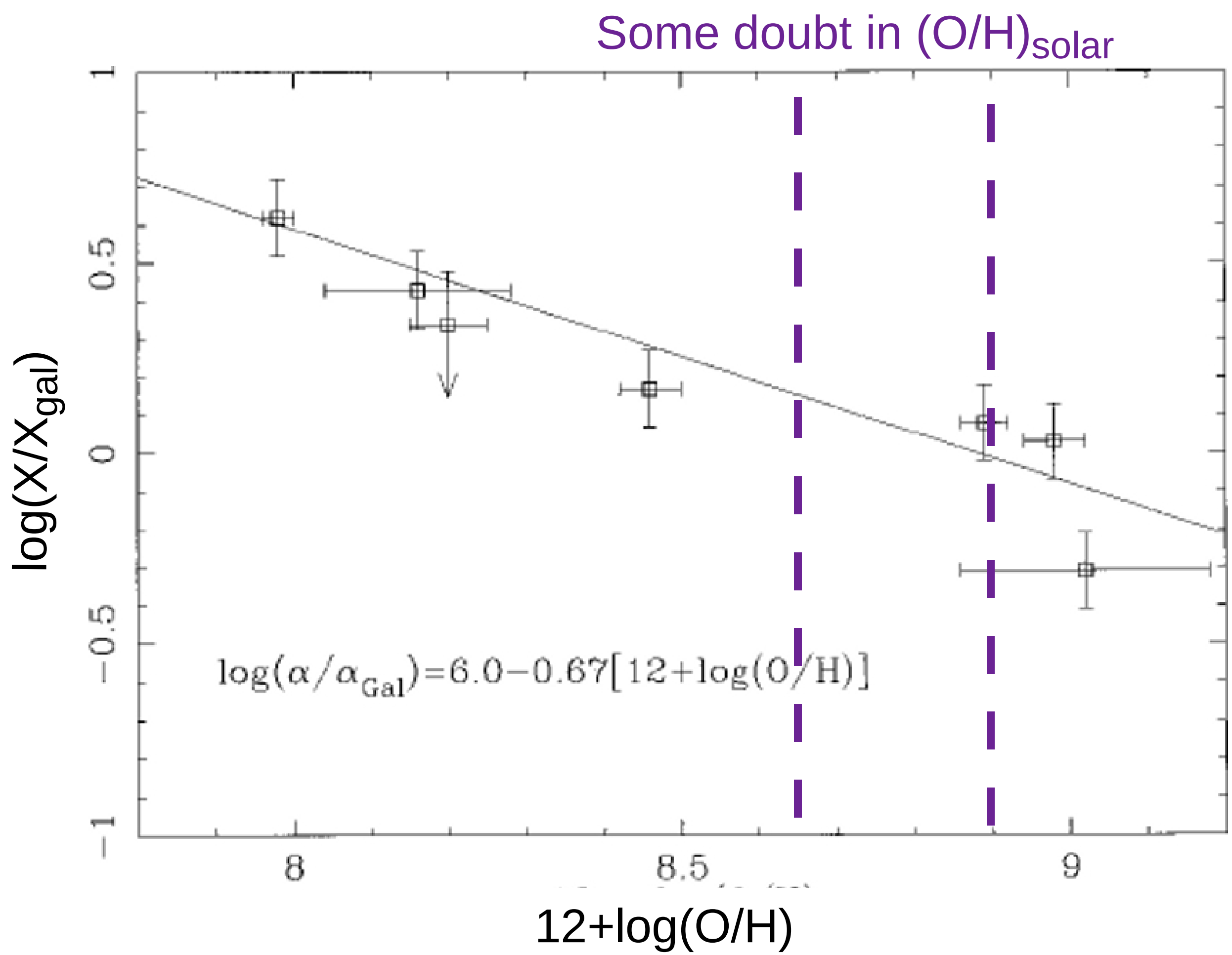

Observationally, resolved CO clouds in Local Group say ***yes*** (Wilson 1995).

Theoretical arguments (e.g., Maloney & Black 1988) also say ***yes.***

Other factors also play a role...

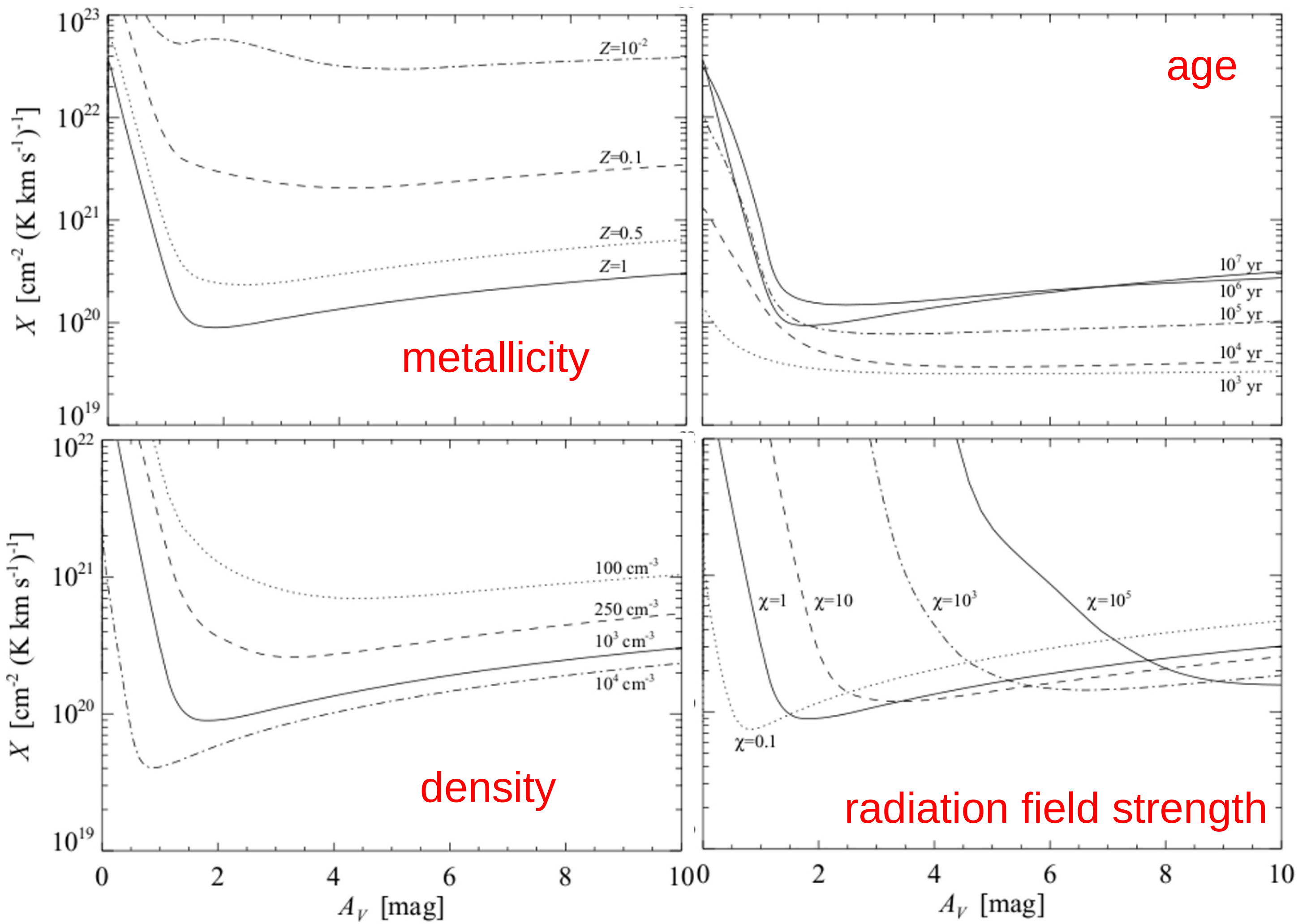

In addition to the dependence of X on O/H and n_e, Bell+ (2006) find variations with time and with radiation field strength! Thus geometry of star-forming regions could be important.

The future with ALMA

PdBI		***ALMA***
		will **boost spatial resolution:**
0.5-2.0” (10-300 pc @5-30 Mpc)	➔	*0.05-0.1” (1-10 pc @5-30 Mpc)*
		boost sensitivity:
$M(H_2)$-3σ [Δv ~ 10km/s@20Mpc]: ~10^5 M_{sun} *in* t_{int}~15-20h	➔	*~10^4 M_{sun} in t_{int}~1.5h*
		improve statistics in the Local Universe (NUGA++?):
12 galaxies at ~0.5” (@5-30Mpc) **200 hrs**	➔	*100-150 galaxies at ~0.1” (@5-30Mpc)* ***200 hrs***

The future with ALMA

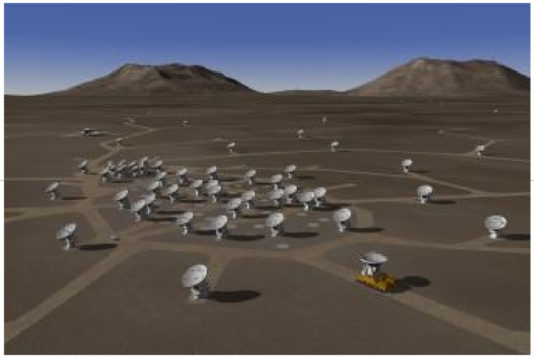

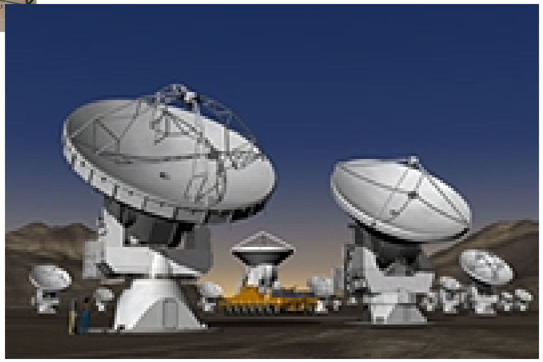

- ✔ ALMA will transform our understanding of how stars form, and how star formation and AGN fueling processes interact -
- ✔ We will be able to perform Galactic-scale science in distant galaxies -
- ✔ The relation between molecules and metal abundance can be explored locally, and linked to star formation at high redshift -